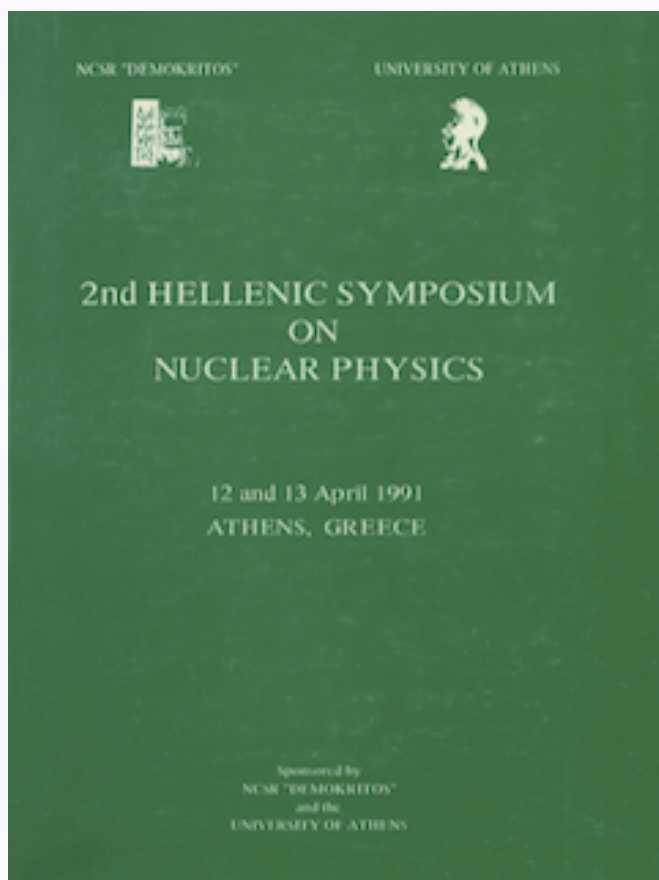


HNPS Advances in Nuclear Physics

Vol 2 (1991)

HNPS1991



COLLECTIVE POTENTIAL FOR HEAVY ION NUCLEAR REACTIONS

C. Syros

doi: [10.12681/hnps.2846](https://doi.org/10.12681/hnps.2846)

To cite this article:

Syros, C. (2020). COLLECTIVE POTENTIAL FOR HEAVY ION NUCLEAR REACTIONS. *HNPS Advances in Nuclear Physics*, 2, 117–167. <https://doi.org/10.12681/hnps.2846>

COLLECTIVE POTENTIAL FOR HEAVY ION NUCLEAR REACTIONS

C. SYROS

Laboratory of Nuclear Technology
University of Patras, GR-26110 Patras, Greece

Abstract

It is shown that the nuclear charge polarisation during heavy ion nuclear reactions enhances the secondary maximum of the collective energy surface and produces a secondary minimum in the deformation energy near $R \simeq R_{\min} + 2\text{fm}$. The potential energy and mass formulas are given as a function of A and Z . It has been shown that charge polarisation without shape deformation and indeed of the prolate type does not produce any secondary minimum. It is also seen that the relativity effect consists in shifting the secondary minimum towards higher rest excentricities. For deformation of the oblate type the collective potential has a similar form like that in the spherical case. Entry and exit channel collective potentials are also given for the case of strong nucleon transfer. The mass for the two-body interacting system has been calculated and for large distances it tends to the corresponding reduced mass. The present theory is based on a particular form of the single particle potential following from the scalar π -meson classical field theory.

1. Introduction

The precise determination of the nuclear collective potential energy for heavy ions is one of the principal problems in the present day nuclear theory. Many authors undertook recently various attempts to establish a viable theory for the heavy ion nuclear interactions with considerable successes [1-7].

Despite the encouraging results the problem continues to be present in the literature [8-14] not only regarding the new experimental results but also the theoretical investigations [16, 17].

The present work is based on an early development [18] in connection with the nuclear structure, radii and binding energies. That theory has been used recently for calculations in fission theory and heavy ion nuclear reactions [2, 15].

The main purpose of the present paper is to generalise previous results [18] and to proceed in deriving various consequences of the theory towards obtaining collective potentials for heavy ion nuclear reactions. Many outstanding problems are still awaiting their solution, the chief of them being the determination of the mass formula which has to be used in solving the classical or the quantum mechanical equations describing the motion of two fusing heavy ions. This problem may appear in a number of different variances and in particular those concerning the spallation, the nuclear fission, the nucleon ejection during fusion, etc.

In addition, as it will be seen later in the present work there is at least one more aspect of an important phenomenon discovered almost one and a half decade ago [19-20] in connection with the existence of the secondary minimum of the potential energy barrier in the fission of the heavy nuclei. It is related to the nuclear charge polarisation which appears during the collision of heavy ions due to the strong Coulomb repulsion in conjunction with the also very strong attraction between a part of the neutrons. This line of thinking might lend a new aspect to the proximity theory of the collective interactions.

In Section 2 the basic theoretical concepts of the present work are formulated in the simplest possible form of a classical field theory. We start with a non-quantised Lagrangian density for the two interacting fields of the nucleons and the π -mesons. The coupling term used here is the scalar one and the π -meson field is, of course, the one component scalar field. The result is a set of two second-order differential equations. The solution of them leads to a multiplicity of polypoles which may successfully represent shape deformations of the interacting nuclei. In the present work, however, only the monopole solution is discussed as in Section 3. Of course, as it was expected, the result to the lowest approximation is equivalent to folding the simple Yukawa potential $\sim e^{-\mu \cdot r}/r$. However, the folding procedure does not lead to results beyond spherical symmetry except in the case in which asymmetry is arbitrarily introduced in the folding density distribution function for the nuclear matter. In Section 4 the results for the collective nuclear potential are given. They are referring to the centric collision of ions with given excentricity and charge polarisation. The effect of the relativistic con-

traction is also discussed. Extensive numerical calculations have been made with a Hewlett-Packard 45b computer. The case of the collision of prolate ellipsoids with non-zero impact parameter is investigated in Section 5. In Section 6 the entrance and exit channel calculations of V_{coll} are briefly discussed, while the ion mass for fusion reactions is given in Section 7. Finally, some conclusions and the discussion of them are given in Section 8.

As the principal result of the present work might be considered the revelation of the double humped collective potential energy surface as a consequence of the shape deformation and the simultaneous nuclear charge polarisation. Another important result is the fact that the shape deformed nuclear potential can be obtained directly from the solution of the resulting Euler-Lagrange field equations for higher order polipoles. A number of useful generalisations of our approach is obvious.

2. THE FUNDAMENTALS OF THE THEORY

Our contribution to the solution of the problem expounded in Section 1 begins with a non-quantised Lagrangian density for the derivation of a single particle nuclear potential. This potential is subsequently used as the basis for the deduction of a collective potential for heavy ion nuclear reactions. Since we consider the heavy ion fusion as the inverse process of the nuclear fission the potential we obtain expresses the features of the shape deformation. The form of the Lagrangian we use is preferable to us because it allows to use the nuclear density matrix in the form of products of normalised Slater determinants, $S_A(x_1, \dots, x_A)$, where the elements of S_A may be appropriate Schrödinger or Dirac single-particle wave functions. Using these Slater determinants we write the Lagrangian density in the form [18]

$$\begin{aligned} \mathcal{L}\left(S_A, \frac{\partial}{\partial x_j} S_A, \Phi, \frac{\partial}{\partial x_j} \Phi\right) = & -\frac{1}{2} S_A^\dagger \left[\sum_j \left(i\gamma_j \frac{\partial}{\partial x_j} + m_j \right) \right] S_A \\ & -\frac{1}{2} \left(\mu^2 \Phi^2 - \sum_j \frac{\partial}{\partial x_j} \Phi \frac{\partial}{\partial x_j} \Phi \right) \\ & - G S_A^\dagger \Gamma \Phi S_A, \end{aligned} \quad (2.1)$$

where, e.g., $i\gamma_j \frac{\partial}{\partial x_j} + m_j$ is the Hamiltonian and

$$\vec{x}_j = \{x_{vj} | j = 1, 2, \dots, A\}$$

the four-vector of the j -th nucleon. The parameter $\mu = 1/r_0$, and r_0 is the nucleon radius. The field Φ will obviously depend on all coordinates $\{x_j = (t, \vec{r}_j)\}$.

The form (2.1) of \mathcal{L} is particularly suitable for the density averaging procedure which we are intending to use subsequently in solving the Euler-Lagrange equations. The variational principle

$$\delta \int dx_1^4 \dots dx_A^4 \mathcal{L} \left(S_A, \frac{\partial}{\partial x_j} S_A, \Phi, \frac{\partial}{\partial x_j} \Phi \right) \quad (2.2)$$

gives rise to the two coupled equations

$$\sum_j \left(i\gamma_j \frac{\partial}{\partial x_j} + m_j \right) S_A = -G \Gamma \Phi S_A \quad (2.3)$$

and

$$\sum_j \square_j \Phi + \mu^2 \Phi = -G S_A^\dagger \Gamma S_A. \quad (2.4)$$

We are interested in solving eq. (2.4) in the time-independent limit and we put $\square \rightarrow -\nabla^2$.

We consider also the simplest case $\Gamma=1$ (scalar coupling) and we use the property

$$\int S_A^\dagger S_A d\vec{r}_2^3 \dots d\vec{r}_A^3 = A^{-1} \sum_{n_\alpha} q_{n_\alpha}(\vec{r}_1), \quad (2.5)$$

where

$$q_{n_\alpha}(\vec{r}_1) = \Psi_{n_\alpha}^\dagger(\vec{r}_1) \cdot \Psi_{n_\alpha}(\vec{r}_1) \quad (2.6)$$

and n_α is a set of one-nucleon quantum numbers.

Thus, we can consider the stationary problem and carry out the reduction of the many-particle problem (2.4) by means of the integration

$$\int \Phi(\vec{r}_1, \dots, \vec{r}_A) d\vec{r}_2^3 \dots d\vec{r}_A^3 = \varphi(\vec{r}_1). \quad (2.7)$$

Next, we exploit the fact that Φ is a fast decreasing function of all $\vec{r}_1, \dots, \vec{r}_A$ and apply the Gauss theorem

$$\begin{aligned} \int \operatorname{div}_j \cdot \operatorname{grad}_j \Phi(r_1, \dots, r_j, \dots, r_A) d\vec{r}_j^3 = \\ = \int \operatorname{grad}_j \Phi(\vec{r}_1, \dots, \vec{r}_j, \dots, \vec{r}_A) \cdot d\vec{A}_j = 0 \end{aligned} \quad (2.8)$$

for $j = 2, 3, \dots, A$.

From (2.4 - 2.8) it follows that

$$\nabla^2 \varphi(\vec{r}_1) - \mu^2 \varphi(\vec{r}_1) = 4\pi g^2 \bar{\varrho}(\vec{r}_1); \quad G = 4\pi g^2, \quad (2.9)$$

where $\bar{\varrho}(\vec{r}_1)$ is the mean nuclear mass density defined through the expression

$$\bar{\varrho}(\vec{r}_1) = A^{-1} \sum_{n_\alpha} \varrho_{n_\alpha}(\vec{r}_1). \quad (2.10)$$

A further simplification is concerning the volume, V , for which the Gauss theorem has been applied in (2.8). The nuclear mass density being approximately constant inside V is put to a first approximation equal to

$$\bar{\varrho}(\vec{r}) \simeq A^{-1} \sum_{n_\alpha} \frac{A}{V} = A^{-1} \cdot \frac{A^2}{V} = \frac{A}{V}. \quad (2.11)$$

From (2.9) and (2.11) we obtain the equations

$$\nabla^2 \varphi_i(\vec{r}) - \mu^2 \varphi_i(\vec{r}) = 4\pi g^2 \frac{A}{V}; \quad 0 \leq r \leq a \quad (2.12)$$

and

$$\nabla^2 \varphi_0(\vec{r}) - \mu^2 \varphi_0(\vec{r}) = 0; \quad a \leq r, \quad (2.13)$$

where a is the radius of the nucleus.

3. THE SINGLE - PARTICLE INTERACTION

The single - particle potential used in the present paper is obtained by solving eqs. (2.12), (2.13) and by taking only the spherically symmetric solution.

It was shown a long time ago that it is possible to derive a single particle central potential [18] which exhibits a characteristic dependence on the mass number, A , of the nucleus. To this purely nuclear potential the Coulomb potential was added and it was, then, used for nuclear structure calculations.

The resulting total potential energy for the interior of the nucleus is given by the simple closed expression

$$V_i(r) = -3g^2/r_0 \left[1 - (1 + A^{1/3}) e^{-A^{1/3}} (r_0/r) \sinh(r/r_0) \right] + \\ + 3Z \cdot e^2/2r_0 \cdot A^{1/3} \cdot \left[1 - (1/3) (r/r_0 A^{1/3})^2 \right]; \quad 0 \leq r \leq a \quad (3.1)$$

and for the outside of the nucleus by

$$V_o(r) = -3g^2/r_0 \left[A^{1/3} e^{A^{1/3}} - (1 + A^{1/3}) \sinh A^{1/3} \right] (r_0/r) e^{-(r/r_0)} + \\ + Z \cdot e^2/r; \quad r \geq a. \quad (3.2)$$

Equations (2.12) - (2.13) may give as solutions all higher order polypoles which are appropriate to the non-spherical nuclei. These, however, are not considered in the present work.

The factor g^2 is the interaction constant of the scalar π -meson and the nucleon fields. The boundary conditions for (2.12) and (2.13) have been taken such that the condition $V_i = V_o$ holds. The form of the above potential is shown in fig. 1 for the nuclei

$${}^{10}_3\text{B}, \quad {}^{128}_{52}\text{Te}, \quad {}^{235}_{92}\text{U}, \quad {}^{500}_{200}\text{X}, \quad {}^{750}_{300}\text{X}.$$

We use the above potential to calculate nuclear deformation energies and collective potentials for interacting heavy ions.

The method used consists in folding the nuclear density of the part of the one nucleus which is outside the rest of the other nucleus with the potential valid for the exterior region, both nuclear and Coulomb. Other authors have also used in connection with (3.1) various folding procedures with great success.

This procedure does not produce a secondary minimum in the potential energy barrier. The way of folding used in the present work is given by

$$V(\vec{R}) = \int_{V_1 - \vec{O}} V_o(\vec{R} + \vec{r}') \cdot \rho(\vec{r}') \cdot d\vec{r}', \quad (3.3)$$

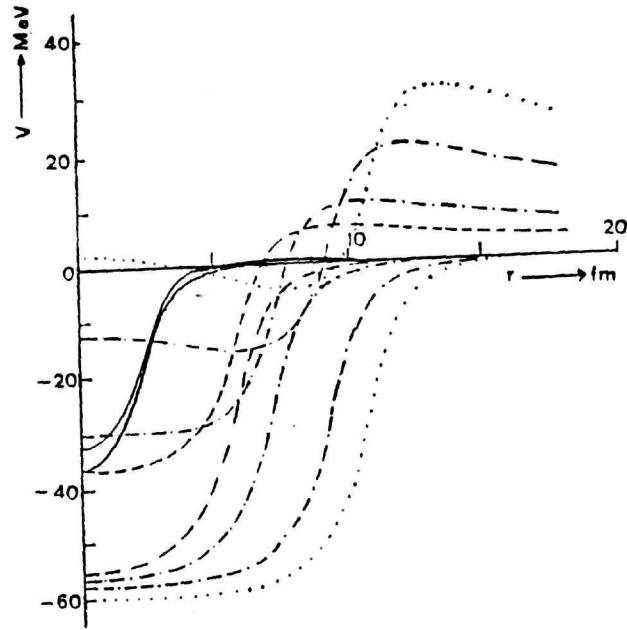


Fig. 1. Single particle potential curves for spherical nuclei according to eqs (3.1) and (3.2) as a function of the distance. The various curves correspond to different mass and proton numbers. The curves for protons intersect the r -axis. A certain form similarity with the Woods-Saxon potential is obvious. The principal characteristic of the present potential is the slope change with the mass number. While the depth increases for neutrons, if the mass number, A , increases, it decreases strongly for increasing proton number, Z . Another important feature is the change of sign in the slope of $V(r)$ in the neighbourhood of $r=0$, if Z increases beyond a certain $Z_0(A)$. Also the slope of $V(r)$ at the boundary of the nucleus increases for increasing mass number. The interaction constant, g , has been given the value $g = 1.92 \cdot 10^{-9}$. The potential energy curves intersect the axis of ordinates from top to bottom in the following order: $^{750}_{300}\text{X}$ (protons), $^{500}_{200}\text{X}$ (protons), $^{235}_{92}\text{U}$ (protons), $^{10}_5\text{B}$ (protons), $^{10}_5\text{B}$ (neutrons), $^{125}_{52}\text{Te}$ (protons), $^{125}_{52}\text{Te}$ (neutrons), $^{235}_{92}\text{U}$ (neutrons), $^{500}_{200}\text{X}$ (neutrons) and $^{750}_{300}\text{X}$ (neutrons).

where $V_1 \gg V_2$ are the initial volumes of the two nuclei, \bar{O} is the common volume of the interacting ions and $\rho(\vec{r})$ the nuclear matter density distribution. Eq. (3.3) yields effectively the potential energy of a fraction of the one nucleus in the field of the other one. In doing the integration in eq. (3.3) we do not consider neither friction or change of the density of the nuclear matter nor angular momentum effects or transfer. This implies that the nucleons accommodate themselves in the increasing volume of the bigger nucleus. The influence of the angular momentum and of the spins of the interacting nuclei on the resulting collective potential energy will be considered elsewhere. \vec{R} is the position vector having its origin at the centre of mass of the one nucleus and pointing to the centre of mass of the other nucleus.

In studying heavy ion reactions one has to answer the question as to the direction of the nucleon transfer. One also has to think about parallel or antiparallel neutron and proton transfer. These questions have been investigated in the present work. The result is summarized in the Fig. 3c which gives the force exercised by each of the ions on protons or neutrons in the critical region of the interaction volume. To find the force on protons we take, as usual, the gradient of the potential energy and we find

$$F(r; A, Z) = \begin{cases} 3g^2 \cdot (1 + A^{1/3}) \cdot e^{-A^{1/3}} \left[\cosh(r/r_0)/(r \cdot r_0) - \sinh(r/r_0)/r^2 \right] - \\ \quad - Z \cdot e^2 \cdot r / (r_0^3 \cdot A); & r \leq r_0 \cdot A^{1/3}, \\ |-\nabla V(r)| = \begin{cases} 3g^2 \cdot [A^{1/3} e^{A^{1/3}} - (1 + A^{1/3}) \sinh A^{1/3}] \cdot e^{-r/r_0} \cdot (1/(r \cdot r_0) + 1/r^2) - \\ \quad - Z \cdot e^2 / r^2; & r \geq r_0 \cdot A^{1/3}. \end{cases} \end{cases} \quad (3.4)$$

If we put $Z = 0$ in eq. (3.4) we get the force acting on the neutrons when they are exactly on the nuclear surface. This force exhibits a sharp maximum just on the nuclear surface (Fig. 2a, b).

From Fig. 2a, b it follows that in the neighbourhood of the nuclear surface there is a shell around the nuclear surface of approximately 3fm thickness, where the force acquires particularly high values (Fig. 2c). In the interior of the nucleus and beyond the spherical shell the force

The single particle nuclear force, $F(r; A, Z)$, as a function of the distance, r , from the centre of nucleus with parameter the mass number for neutrons (a) and for protons (b). The maximum of the force is at $r=r_0 A^{1/3}$ both for neutrons and protons. The curve shows a resonance-like form of which the FWHM is about 2 fm. This implies that an exceedingly strong force acts on the nucleons on the nuclear surface (c), whilst the rest of the nucleons are quasi-free. This strong surface force gives rise to the formation of a shell of strongly attracted nucleons which compress the rest of the nucleons inside the nucleus. Considering that the ratio A_s/A is a rather small number, where A_s the number of the nucleons inside the strong force shell, we see that it is consistent with the independent particle model. Using the surface force one easily calculates the classical surface tension as well as the pressure inside the nucleus.

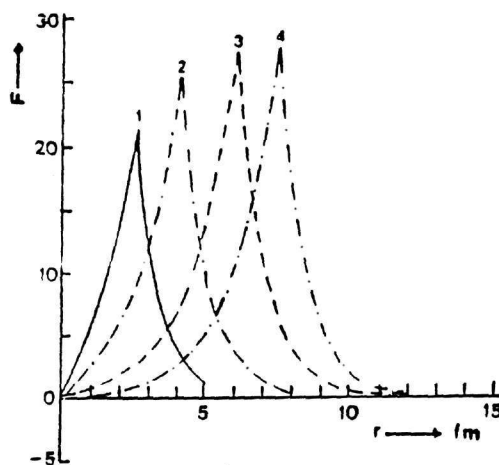


Fig. 2a.

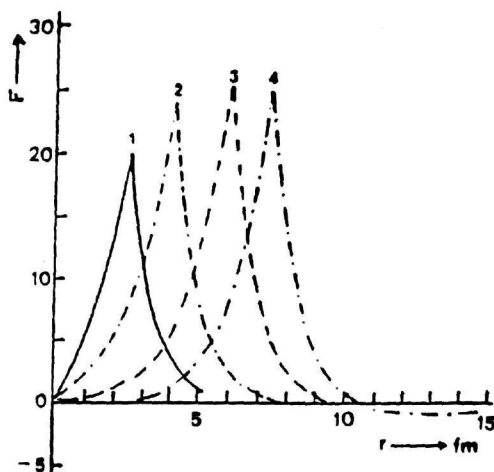


Fig. 2b.

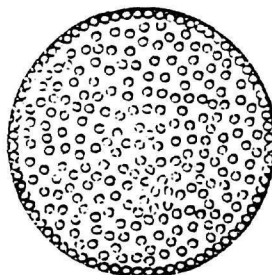


Fig. 2c.

on the nucleons is considerably weaker and tends exponentially to zero with increasing distance from the surface.

The situation arising is reminiscent of a gas of almost free nucleons which are compressed by a spherical layer of nucleons.

If the mass number, A , is very high, then the ratio A_s/A , where A_s is the number of the nucleons on the surface, is very small. This might give some explanation for the success of the independent particle model. The majority of the nucleons are moving quasi-free in the nucleus inside a nuclear «wall» kept by the strong central surface force.

From eq. (3.4) we can gain still more information about the heavy ion nuclear reactions. To this end let us take the derivative of F with respect to the mass number in the neighbourhood of the nuclear surface. The result is :

$$\left. \frac{\partial}{\partial A} F_\alpha(r, A, Z) \right|_{r=r_0 A^{1/3} + \lambda r_0} = \begin{cases} g^2 \cdot A^{-2/3} e^{-A^{1/3}} / (r_0^2 \cdot (\lambda + A^{1/3})) \cdot \left\{ (-A^{1/3}) (\cosh(\lambda + A^{1/3}) - \sinh(\lambda + A^{1/3}) / (\lambda + A^{1/3})) + (1 + A^{1/3}) \cdot (\sinh(\lambda + A^{1/3}) - 2 \cdot \cosh(\lambda + A^{1/3}) / (\lambda + A^{1/3}) + 2 \sinh(\lambda + A^{1/3}) / (\lambda + A^{1/3})^2) \right\} \\ + Z \cdot e^2 / r_0^2 \cdot (2 \cdot A^{-3/3} / 3 + \lambda \cdot A^{-2}); \quad \alpha = i; \quad \lambda < 0 \\ \\ g^2 \cdot A^{-2/3} e^{-(\lambda + A^{1/3})} / (r_0^2 \cdot (\lambda + A^{1/3})) \cdot \left\{ A^{1/3} \sinh(A^{1/3}) + e^{A^{1/3}} - (1 + A^{1/3}) \cosh(A^{1/3}) + (e^{A^{1/3}} - A^{1/3} \cdot e^{A^{1/3}} - (1 + A^{1/3}) \cosh(A^{1/3}) + \sinh(A^{1/3}) + 2 \cdot A^{1/3} \sinh(A^{1/3})) / (\lambda + A^{1/3}) + (2 \cdot (1 + A^{1/3}) \sinh(A^{1/3}) - 2 \cdot A^{1/3} e^{A^{1/3}}) / (\lambda + A^{1/3})^2 \right\} + 2 Z e^2 A^{-3/3} / (3 r_0^2 (\lambda + A^{1/3})^3); \quad \alpha = o; \quad \lambda > 0 \end{cases} \quad (3.5)$$

In eq. (3.5) $\lambda > 0$ ($\lambda < 0$) means that the derivative of the force is taken outside (inside) the nucleus.

Equating $\left. \frac{\partial F_\alpha}{\partial A} \right|_{r=\bar{r}} = 0$ gives the critical value of $A_c(Z)$ for protons ($Z > 0$) and for neutrons ($Z = 0$) for which the resultant force at the

The force acting on the nucleons in the neighbourhood of the nuclear surface as a function of the mass number having as a parameter the number of protons, Z . For neutrons ($Z=0$) (a) the force is generally higher than for protons ($Z>0$) (b). The three curves α , β , γ give the force on three different surfaces: (a) corresponds to $r = a + 2r_0$ (a = radius), (β) to $r = a$ and (γ) to $r = a - 2r_0$. It is important to note that the force exactly on the nuclear surface is a monotonically increasing function of the mass number both for neutrons and protons. In the neighbourhood of the nuclear surface this ceases to be anymore the case. This fact complicates the determination of the direction of the nucleon transfer during the heavy ion nuclear reactions.

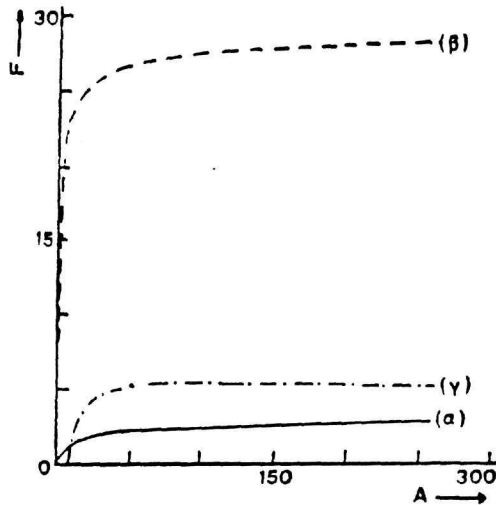


Fig. 3a.

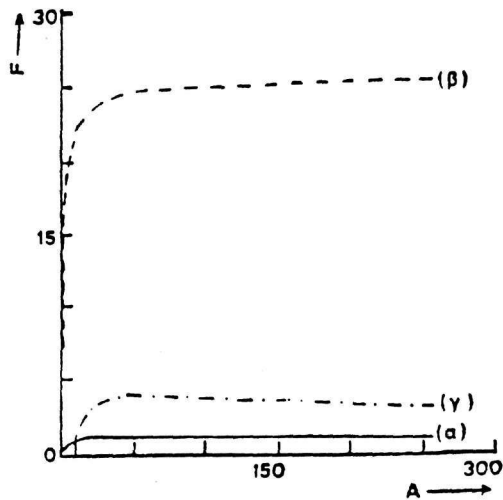


Fig. 3b.

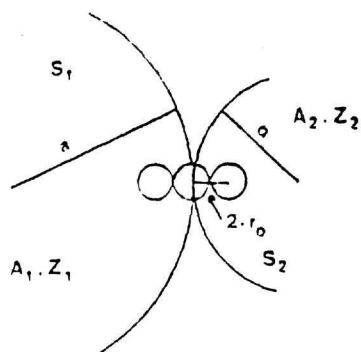


Fig. 3c.

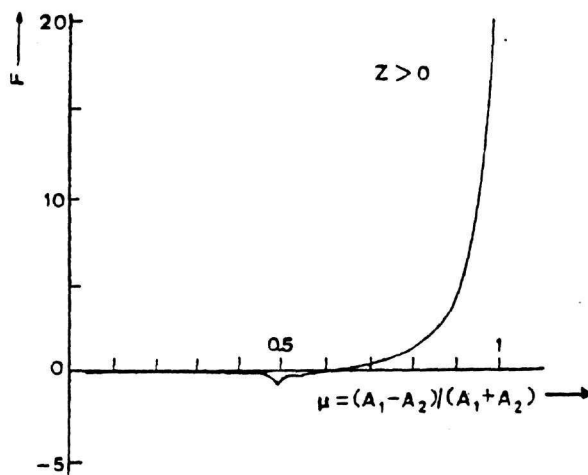


Fig. 3d.

The nucleon transfer criterion (c) is shown also for protons (d) with the detail (e) and for neutrons (f). It is seen that the force directing the nucleon transfer becomes positive after a certain mass number, A_c , or mass asymmetry $(\Lambda_1 - \Lambda_2) / (\Lambda_1 + \Lambda_2)$. For larger values of the mass number, $A > A_c$, the nucleon transfer force (f) is constantly \rightarrow

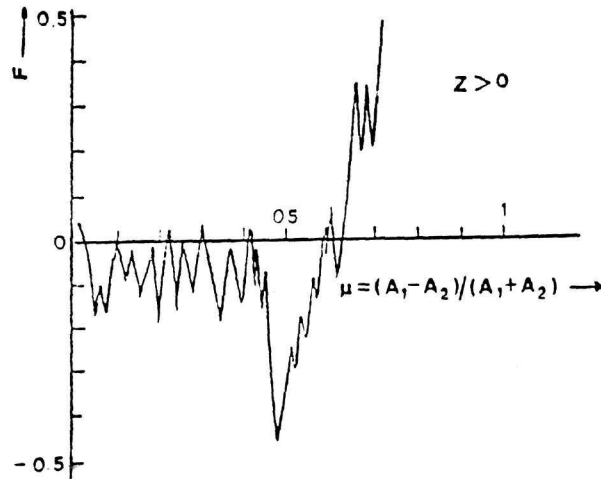


Fig. 3e.

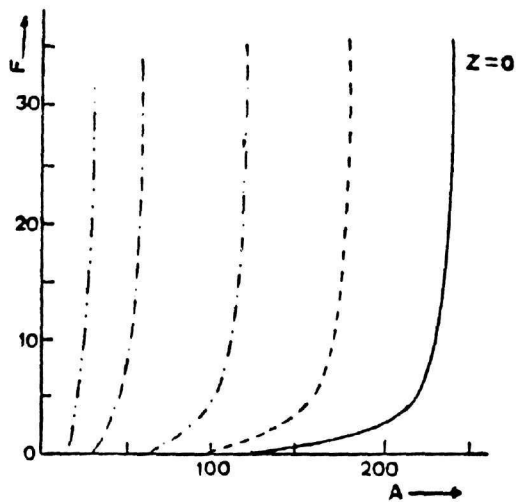


Fig. 3f.

- directed towards the heavier ion. For $A < A_c$ the force is very weak and mainly directed towards the smaller ion with several exceptions capable of causing nucleon oscillations. This curve corresponds to stable nuclei. For non-stable nuclei the situation changes drastically. In intervals of $t \cong 0$ the nucleon transfer may become stochastic.

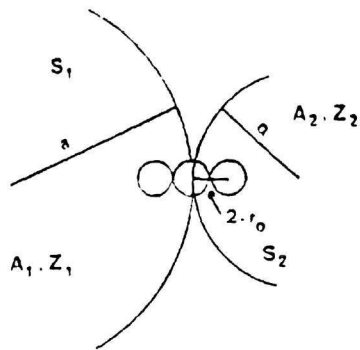


Fig. 3c.

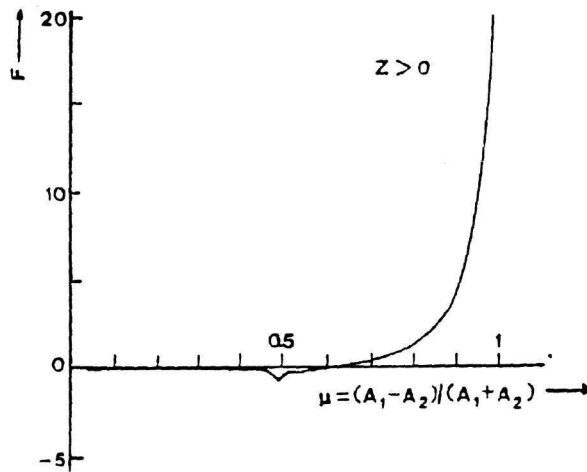


Fig. 3d.

The nucleon transfer criterion (c) is shown also for protons (d) with the detail (e) and for neutrons (f). It is seen that the force directing the nucleon transfer becomes positive after a certain mass number, A_c , or mass asymmetry $(A_1 - A_2) / (A_1 + A_2)$. For larger values of the mass number, $A > A_c$, the nucleon transfer force (f) is constantly \rightarrow

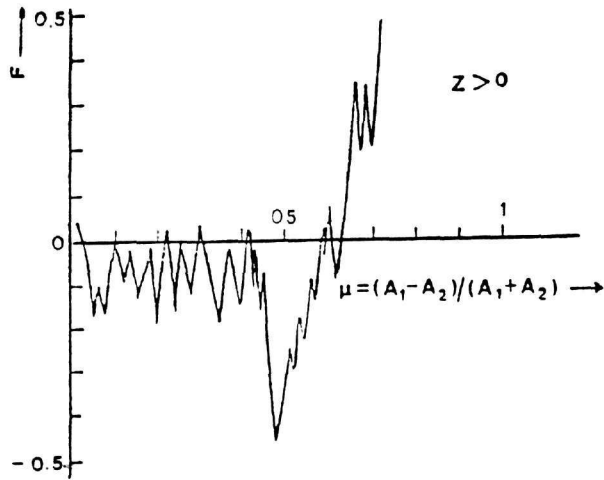


Fig. 3e.

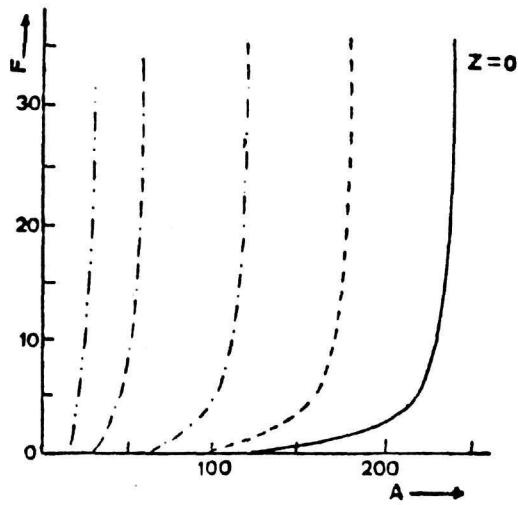


Fig. 3f.

→ directed towards the heavier ion. For $A < A_c$ the force is very weak and mainly directed towards the smaller ion with several exceptions capable of causing nucleon oscillations. This curve corresponds to stable nuclei. For non-stable nuclei the situation changes drastically. In intervals of $t \cong 0$ the nucleon transfer may become stochastic.

considered point ($\vec{r} = r_0 A^{1/3} + \lambda r_0$) changes direction with increasing mass number.

More precisely we have the following behaviour of the nuclear force :

$$F_2(r; A, Z) = \begin{cases} \text{increasing function of } A \text{ for} \\ \text{increasing } A < A_c(Z) \text{ for all values of } r. \\ \text{decreasing function of } A \text{ for} \\ \text{increasing } A > A_c(Z) \text{ at points } r \neq a. \end{cases} \quad (3.6)$$

Considering eq. (3.6) we construct the following nucleon transfer criterion, f , for determining towards which of the two ions is the motion of the transferred nucleons during partial or complete fusion reactions. It is defined by

$$f(A_1, A_2, Z_1, Z_2) = [F_1(a; A_1, Z_1) - F_1(a, A_2, Z_2)] + [F_0(a+2 \cdot r_0; A_1, Z_1) - F_1(a-2 \cdot r_0; A_2, Z_2)] + [F_1(a-2 \cdot r_0; A_1, Z_1) - F_0(a+2 \cdot r_0; A_2, Z_2)]. \quad (3.7)$$

The expression for f gives the resultant of the forces acting on a chain of three nucleons (Fig. 3c-f). These three nucleons occupy the critical contact region of the ions where the nucleon transfer is initiated (Table I).

The nucleon transfer criterion has been evaluated for the case of $A_1 + A_2 = A$ const. and $Z_1 + Z_2 = Z$ constant. The result is shown in Fig. 3d. In defining f the convention has been adopted that positive values imply nucleon transfer from (A_2, Z_2) towards (A_1, Z_1) while negative values indicate the contrary ($A_1 > A_2$ and $Z_1 > Z_2$).

The change of sign of the nucleon transfer criterion implies the existence of oscillations in the mass number space. The relationship between the nucleon transfer and the mass number oscillations and their physical significance will be discussed elsewhere.

Another factor causing deformation of the two interacting nuclei is the differential action of the nuclear and the Coulomb forces. While the protons belonging to the two nuclei repel each other and their motion becomes decelerated when the repulsion becomes too strong, the corresponding neutrons attract each other stronger and stronger and their motion becomes accelerated. This leads to a pronounced deformation of the colliding nuclei which eventually take on an ellipsoidal form.

TABLE I

Some extreme values of the force as function of the mass and atomic numbers, A and Z . The force acting on the neutrons is constantly directed towards the bigger nucleus for distances satisfying $r > -0.5r_0$ ($r > 0$ for the exterior, $r < 0$ for the interior of the nuclear surface). For $r < -0.5$ there exists a maximum of the force at the indicated mass numbers. For protons there exist also maxima at the relevant distances from the nuclear surface for the indicated nuclides. The existence of a maximum implies the change of force direction acting on the nucleons in the neighbourhood of the nuclear surface between two interacting ions (see also Fig. 2).

Distance from nuclear surface in r_0 - units	Position of the force maximum			Normalised absolute maximum value of the force		Absolute value of the force for $\max\{A\}$ and $\max\{Z\}$	
	$A(Z=0)$	A	Z	Neutrons	Protons	Neutrons	Protons
+2.0	—	62	28	2.801	1.315	2.801	1.025
+1.5	—	170	68	4.944	3.086	4.944	2.936
+1.0	—	170	68	8.770	6.570	8.770	6.480
+0.5	—	248	96	15.644	13.106	15.644	13.010
0.0	—	170	69	28.090	25.200	28.090	25.027
-0.5	—	62	28	18.194	15.960	18.194	15.370
-1.0	118	62	28	11.926	10.215	11.831	9.248
-1.5	100	62	28	7.894	6.490	7.726	5.383
-2.0	104	62	28	5.231	4.064	5.068	2.965

Contrary to this deformation is acting the relativistic contraction. If no nuclear charge polarisation is assumed, then the collective potential shows only one single minimum. However, while the ions proceed to the collision, the protons of them show a certain «unwillingness» to follow the neutrons. As a consequence, while the distance of the two nuclear matter centres becomes smaller and smaller, the distance of the two nuclear charge centres may decrease slower than the distance of the mass centres until it suddenly becomes zero. At this point the charge in the compound nucleus acquires again a more or less uniform distribution.

This process may be described by a polarisation function, $\vec{P}(\vec{R})$, for the nuclear charge which is calculated in the next section.

4. THE CHARGE POLARISATION IN CENTRIC COLLISION

The most important feature of the present theory is the introduction of the polarisation function, $\vec{P}(\vec{R})$, in the collective potential. We define the polarisation by the expression

$$\vec{P}(\vec{R}) = \int_{v_1+\vec{0}} \vec{r} \cdot \rho_{c_1}(\vec{r}) \cdot d\vec{r} + \int_{v_2+\vec{0}} \vec{r} \cdot \rho_{c_2}(\vec{r}) \cdot d\vec{r}, \quad (4.1a)$$

where $\rho_{c_1}(\vec{r})$ and $\rho_{c_2}(\vec{r})$ are the charge density distributions of the two ions.

To clarify the physical conditions for which the charge polarisation inside the interacting ions takes place the following different cases are considered:

- (i) If the heavy ions are in sufficient distance from each other and they already interact through the Coulomb potential, the protons show a tendency to occupy the farthest parts of them. Therefore, the average charge distance, R_c , entering the Coulomb potential is bigger than the distances of the centres of the nuclear masses. It is given by

$$R_c = R + P(R), \quad (4.1)$$

where $P(R) = [3r_0/8 \cdot (1 - \epsilon^2)^{-1/3} (A_1^{1/3} + A_2^{1/3})]$

and ϵ is the excentricity of the heavy ions. The absolute value, P , of the polarisation is used due to rotational symmetry. These equations result from the reasonable assumption that the protons occupy the farrest parts of the two ion volumes together with an adequate number of neutrons. The excentricity used to express the form of the interacting ions is for prolate ellipsoids defined as usual by $\epsilon = \sqrt{1 - \frac{b^2}{a^2}} = \sqrt{1 - \frac{\beta^2}{\alpha^2}}$ and is in the present work assumed to be the same for both ions. However, there is no difficulty in introducing two different excentricities or even completely different triaxial ellipsoids. Here and throughout this work we use the notation $\{A_1, Z_1, a, b\}$ and $\{A_2, Z_2, \alpha, \beta\}$ to express the mass number, the atomic number, the large semi-axis and the minor semi-axis of the bigger and the smaller ellipsoids respectively.

- (ii) If the nuclear interaction starts, nucleons pass from the smaller to the bigger heavy ion with the consequence that the half axes of the latter increase. In this case the polarisation function is obtained after some calculations and is given by

$$P(R) = [3r_0/8] \cdot [\alpha_1(R) + (1 - \epsilon^2)^{-1/3} A_2^{1/3}]. \quad (4.2)$$

The function $\alpha_1(R)$ is a solution of the equation

$$x^4 + c_3 \cdot x^3 + c_2 \cdot x^2 + c_0 = 0. \quad (4.3)$$

Eq. (4.3) is a consequence of the nucleon number conservation during fusion and the assumption that the nuclear matter density remains essentially unchanged. The coefficients of the polynomial are given functions of the distance, R , of the ion centres and are given by the expressions

$$\left. \begin{aligned} c_0 &= -(16/3r_0) \cdot A_1 \cdot R - (8/3r_0) \cdot A_2 \cdot R + A_2^{4/3} - \\ &\quad - (1/3r_0^3) \cdot R^4 + (2/r_0^3) \cdot A_2^{2/3} \cdot R^2 \\ c_1 &= 0 \\ c_2 &= 2 \cdot [(R/r_0)^2 - A_2^{2/3}] \\ c_3 &= (8/3r_0) \cdot R \end{aligned} \right\} \quad (4.4)$$

- (iii) If the nuclear interaction has advanced at a stage in which the remaining volume of the smaller heavy ion cannot accommodate Z_1 protons, charge transfer sets in from the smaller to the bigger heavy ion. In this case the charge polarisation weakens, but the proton charge centres change their positions during the fusion reaction in the same way as in case (ii) above.
- (iv) If the fusion process of the heavy ion has arrived at a stage in which the remaining volume of the smaller ion is too small to contain any protons, the polarisation disappears suddenly. The polarisation function equals zero and the distance of the nuclear matter centres is given by

$$R_c = R + Q(R), \quad (4.5)$$

where

$$Q(R) = d_1(R) + d_2(R). \quad (4.6)$$

If it happens that the inequality is satisfied

$$R^2 - \alpha_1^2(R) + \alpha^2 > 0,$$

then $d_1(R)$ and $d_2(R)$ are given by

$$d_1(R) = (A + B) / C \quad \text{and} \quad d_2(R) = (D + E) / F, \quad (4.7)$$

where the quantities A, B, C, D, E, F are also functions of the distance R and are given by

$$A = \left(R - (3/8R) \cdot (2\alpha \cdot R + R^2 - \alpha_1^2(R) + \alpha^2)^2 / (4\alpha \cdot R + R^2 - \alpha_1^2(R) + \alpha^2) \right) \cdot \\ \left(2\alpha^3/3 + (\alpha_1^2(R)\alpha^2 - \alpha^4 - \alpha^2 R^2) / 2R + (R^3 - \alpha_1^2(R) + \alpha^2)^2 / 24 \cdot R^3 \right), \quad (4.8)$$

$$B = (3/8R) \cdot (2R \cdot \alpha_1(R) + \alpha_1^2(R) - \alpha^2 + R^2)^2 / (4\alpha_1(R) \cdot R + \alpha_1^2(R) - \\ - \alpha^2 + R^2) \cdot \left(2\alpha_1^3(R)/3 + (\alpha_1^4(R) \cdot \alpha^2 - \alpha_1^4(R) - R^2 \cdot \alpha_1^2(R)) / (2R) + \right. \\ \left. + (\alpha_1^2(R) - \alpha^2 + R^2)^3 / 24 \cdot R^3 \right), \quad (4.9)$$

$$C = 4 \cdot \alpha_1^3(R) / 3 - \left(2 \cdot (\alpha_1^3(R) + \alpha^3) / 3 + (2 \cdot \alpha^2 \cdot \alpha_1^2(R) - 2 \cdot \alpha_1^2(R) \cdot R^2 - \right. \\ \left. - 2\alpha^2 \cdot R^2 - \alpha_1^4(R) - \alpha^4) / 4R + R^3 / 12 \right), \quad (4.10)$$

$$D = (3(1 - \epsilon^2) / 8 \cdot R) \cdot (\alpha^2 + 2\alpha \cdot R + R^2 - \alpha_1^2(R))^2 / (\alpha^2 + 4\alpha \cdot R + R^2 - \alpha_1^2(R)) \cdot \\ (2 \cdot \alpha^3/3 + (\alpha^2 \cdot \alpha_1^2(R) - \alpha^4 - \alpha^2 R^2) / 2 \cdot R + (R^3 - \alpha_1^2(R) + \alpha^2)^2 / 24 \cdot R^3), \quad (4.11)$$

$$E = (1 - \varepsilon^2) \cdot \left(R - (3/8R) (2 \cdot R \cdot \alpha_1(R) + \alpha_1^2(R) - \alpha^2 + R^2) / (4\alpha_1(R) \cdot R + \alpha_1^2(R) - \alpha^2 + R^2) \right) \cdot \left(2 \cdot \alpha_1^3(R) / 3 + (\alpha^2 \cdot \alpha_1^2(R) - \alpha_1^4(R) - R^2 \cdot \alpha_1^2(R)) / 2R + (\alpha_1^2(R) - \alpha^2 + R^2)^3 / 24 \cdot R^3 \right), \quad (4.12)$$

$$F = (4r_0^3 \cdot A_2) / 3 - (1 - \varepsilon^2) \left(2(\alpha_1^3(R) + \alpha^3) / 3 + (2 \cdot \alpha^2 \cdot \alpha_1^2(R) - 2 \cdot \alpha_1^4(R) - 2R^2 \cdot \alpha_1^2(R) - 2\alpha^2 \cdot R^2 - \alpha_1^4(R) - \alpha^4) / 4R + R^3 / 12 \right). \quad (4.13)$$

On the contrary, if the inequality is valid

$$\alpha_1^2(R) - \alpha^2 - R^2 \geq 0, \quad (4.14)$$

then eqs. (4.7) change and become

$$d_1(R) = (A - B) / C \quad \text{and} \quad d_2(R) = (D - E) / F. \quad (4.15)$$

In this case the quantities A, B, C, D, E, F are given by the expressions

$$A = (3/8R) (2R \cdot \alpha_1(R) + \alpha_1^2(R) - \alpha^2 + R^2)^2 / (4R \cdot \alpha_1(R) + \alpha_1^2(R) - \alpha^2 + R^2) \cdot \left(2\alpha_1^3(R) / 3 + (\alpha^2 \cdot \alpha_1^2(R) - \alpha_1^4(R) - \alpha_1^2(R) \cdot R^2) / 2R + (\alpha_1^2(R) - \alpha^2 + R^2)^3 / 24 \cdot R^3 \right), \quad (4.16)$$

$$B = (3/8R) (2R \cdot \alpha + R^2 - \alpha_1^2(R) + \alpha^2)^2 / (4\alpha \cdot R + R^2 - \alpha_1^2(R) + \alpha^2) \cdot \left(2 \cdot \alpha^3 / 3 + (\alpha^2 \cdot \alpha_1^2(R) - \alpha^4 - \alpha^2 \cdot R^2) / 2R + (R^2 - \alpha_1^2(R) + \alpha^2)^3 / 24 \cdot R^3 \right), \quad (4.17)$$

$$C = (4 \cdot \alpha_1^3(R) / 3) - \left(2(\alpha^3 + \alpha_1^3(R)) / 3 + (2\alpha^2 \cdot \alpha_1^2(R) - 2R^2 \cdot \alpha_1^2(R) - \alpha^4 - 2\alpha^2 \cdot R^2 - \alpha_1^4(R)) / 4R + R^3 / 12 \right), \quad (4.18)$$

$$D = (3(1 - \varepsilon^2) / 8R) (2\alpha \cdot R + R^2 - \alpha_1^2(R) + \alpha^2)^2 / (4\alpha \cdot R + R^2 - \alpha_1^2(R) + \alpha^2) \cdot \left(2 \cdot \alpha^3 / 3 + (\alpha^2 \cdot \alpha_1^2(R) - \alpha^4 - \alpha^2 \cdot R^2) / 2R + (R^2 + \alpha^2 - \alpha_1^2(R))^3 / 24 \cdot R^3 \right), \quad (4.19)$$

$$E = (1 - \varepsilon^2) \left(3/8R \cdot (2R \cdot \alpha_1(R) + \alpha_1^2(R) - \alpha^2 + R^2)^2 / (4R \cdot \alpha_1(R) + \alpha_1^2(R) - \alpha^2 + R^2) - R \right) \left(2\alpha_1^3(R) / 3 + (\alpha^2 \cdot \alpha_1^2(R) - R^2 \cdot \alpha_1^2(R) - \alpha_1^4(R)) / 2R + (\alpha_1^2(R) - \alpha^2 + R^2)^3 / 24 \cdot R^3 \right), \quad (4.20)$$

$$F = 4r_0^3 \cdot A_2 / 3 - (1 - \varepsilon^2) \left(2(\alpha_1^3(R) + \alpha^3) / 3 + (2\alpha^2 \cdot \alpha_1^2(R) - 2R^2 \cdot \alpha_1^2(R) - \alpha^4 - 2\alpha^2 \cdot R^2 - \alpha_1^4(R)) / 4R + R^3 / 12 \right). \quad (4.21)$$

The relations (4. 6) - (4. 21) follow from geometrical considerations on the basis of Fig. 4 and from the fact that complete fusion of the ions takes place with nucleon transfer from the small to the big ion. This is not an assumption but the result of the calculation of the force responsible for the nucleon transfer. It is evident that the nucleons likely to be transferred from one to the other ion must necessarily be on the nuclear

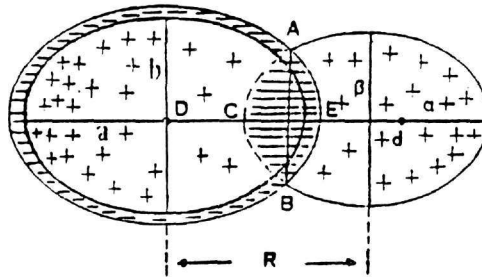


Fig. 4. Collision of two deformed heavy ions with impact parameter equal to zero. The initial values of the semi-axes fulfill the conditions $a > \alpha$, $b > \beta$. The fact that nucleons move from the smaller to the bigger ion is used to calculate the increasing axes $2a(R)$, $2b(R)$ with diminishing R . The initial volumes of the ions are V_1 and V_2 , $V_1 > V_2$. The common volume is AEBC. The volume of the smaller ellipsoid AEBC determines the transfer of nucleons which are distributed uniformly inside the bigger ellipsoid (shaded volume). The shaded volume increases with decreasing centre distance, R . D and d are the centres of the nuclear masses.

surface. But exactly on the nuclear surface the force is a strictly increasing function of the mass number. The effective force responsible for the actual nucleon transfer equals the difference of the forces by the two interacting ions on their common surface.

The polarisation function $P(\vec{R})$ as defined here represents a length which is added to the distance of the nuclear mass centres, R , to give the average distance of the proton charge centres entering the Coulomb potential. It is illustrated in Fig. 5 for a pair of ions $^{257}_{102}\text{No} - ^{243}_{93}\text{Am}$.

In calculating the collective potential energy, $V_{\text{coll}}(R)$, the potential energy of each of the ions in the field of the other ion should be determined. In doing so one is tempted to take the half of the sum for reason of symmetrisation. However, the argumentation just given above shows that this should not be done due to the inequality (Fig. 3a, b(β)).

$$|\text{grad } V_1(r)|_{r=a} > |\text{grad } V_2(r)|_{r=a} \quad (4.22)$$

It is, therefore, seen that nucleon transfer takes place generally easier from the nucleus with smaller A_2 to the nucleus with larger A_1 than conversely ($A_1 > A_2$). This happens because the nucleon attraction is stronger towards the surface of the heavier ion as inequality (4.22) shows. If the mass numbers A_1 and A_2 of the ions before the interaction are different, then, of course, it is not allowed to symmetrize the collective potential energy because of the effect just mentioned. In this case the half axes of the bigger nucleus increase. For spherical nuclei the radius, R_1 , will take the final value $R_{1f} = (A_1 + A_2)^{1/3} r_0$, if no nucleon emission accompanies the fusion process. In any other case, e.g., of scattering, nuclear reaction or spallation, the final value of the radius, R_1 , will be smaller than R_{1f} associated with no nucleon emission.

The collective potential energy obtained in the above way has the following forms corresponding to the clarifications given in the equations (4.1) - (4.5). Thus, we have :

$$(i): V_{\text{coll}} = (-3g^2 \cdot A_2)/r_0 \left(A_1^{1/3} e^{A_1^{1/3}} - (1 + A_1^{1/3}) \sinh A_1^{1/3} \right) e^{-R/r_0} / (R/r_0) + (Z_1 \cdot Z_2 \cdot e^2) / (R + R_c) \quad (4.23)$$

$$(ii): V_{\text{coll}} = (-3g^2 (A_2 - A_2'))/r_0 \left((A_1 + A_2')^{1/3} e^{(A_1 + A_2')^{1/3}} - (1 + (A_1 + A_2')^{1/3}) \sinh (A_1 + A_2')^{1/3} \right) \cdot e^{-(R+d_2(R))/r_0} / ((R+d_2(R))/r_0) + (Z_1 \cdot Z_2 \cdot e^2) / (R + R_c), \quad (4.24)$$

where the nucleon transfer from A_2 to A_1 at each distance is given as a function of this distance by

$$A_2' = (3(1 - \varepsilon^2)/r_0^3) \left(2(\alpha_1^3(R) + \alpha^3)/3 + (2 \cdot \alpha^2 \cdot \alpha_1^2(R) - 2R^2 \cdot \alpha_1^2(R) - 2\alpha^2 \cdot R^2 - \alpha_1^4(R) - \alpha^4)/4R + R^3/12 \right). \quad (4.25)$$

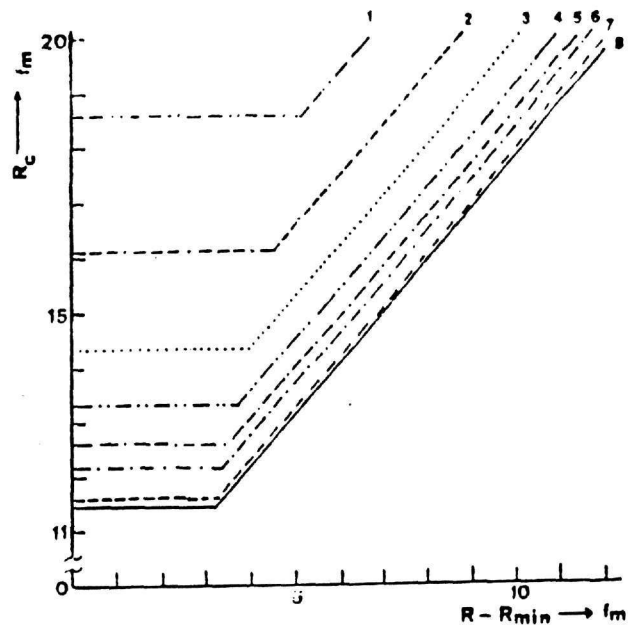


Fig. 5a.

Nuclear charge polarisation as a function of the distance of the ion centres. It is defined as the distance of the charge centres of the fusing ions. The axis of abscissae gives the difference $R - R_{\min}$, where R_{\min} is the value of R for which the one ion is absorbed by the other. In the last stage of the fusion the charge distance remains almost constant until it vanishes suddenly. As it is expected the charge polarisation implies the slower decrease of the distance of \rightarrow

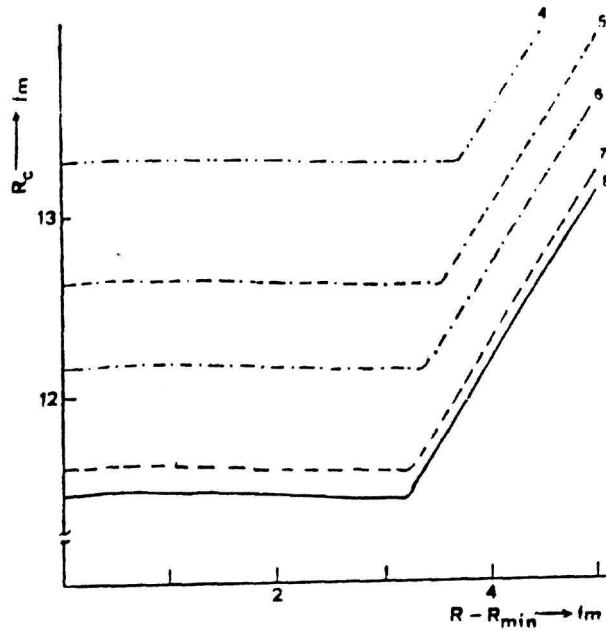


Fig. 5b.

- the two charge centres with decreasing R . At very small distances the charge transfer sets in, but the distance of the charge centres remains almost constant until finally it vanishes completely. The curves are for the pair $^{257}_{102}\text{No} - ^{248}_{95}\text{Am}$, and 1-8 correspond to the eccentricities $\epsilon = 0.875, 0.8, 0.7, 0.6, 0.5, 0.4, 0.2, 0.0$ (a). In (b) the curves represent a detail of (a). It is seen that there is a small variation in horizontal part with varying R .

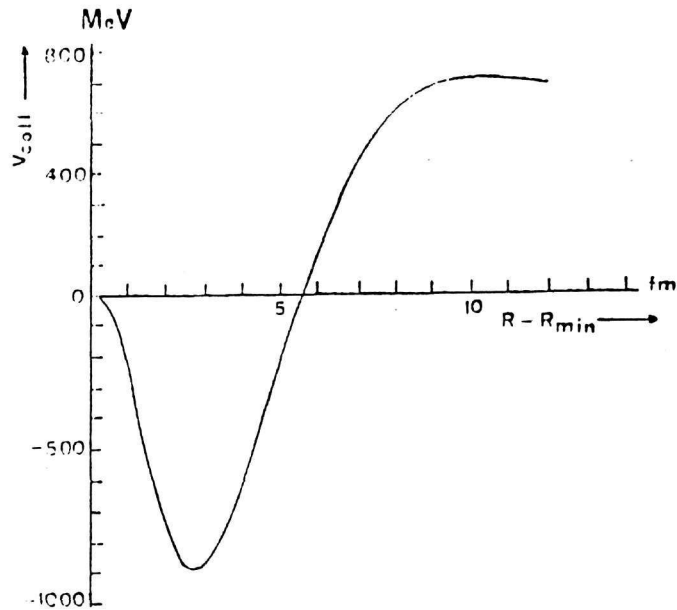
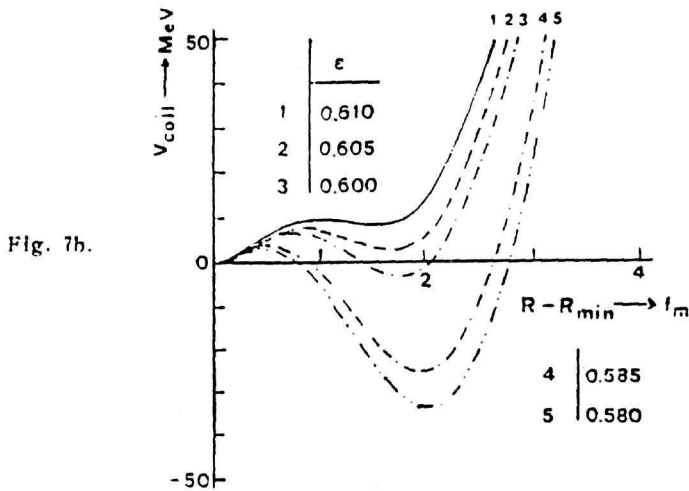
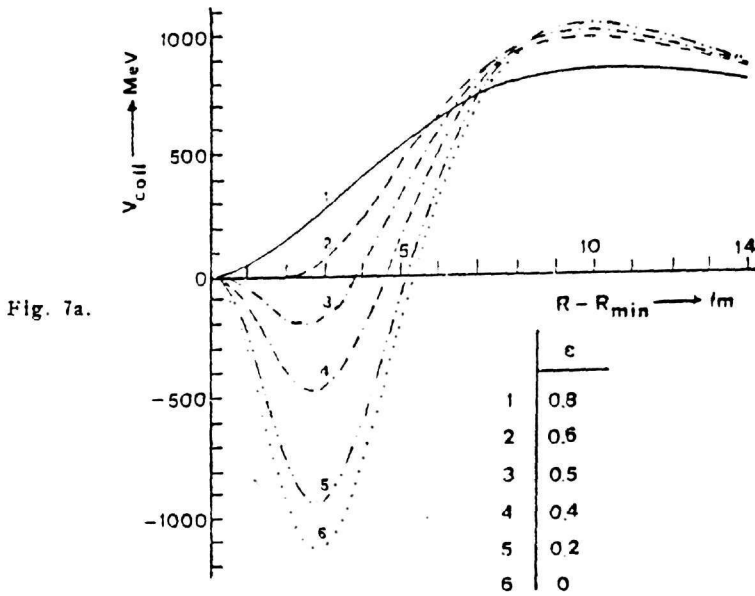


Fig 6. Collective potential energy of the fusing heavy ion system $^{257}_{102}\text{No} - ^{248}_{95}\text{Am}$ as function of the centre of masses distance, R . The ions are considered as spherical ($\epsilon = 0$) but the nuclear charge distribution densities in their interiors are not uniform ($\rho \neq 0$). Under the conditions stated the potential energy surface exhibits a single minimum due to the nuclear attraction and a single maximum due to the Coulomb repulsion. After the beginning of the fusion the distance is measured between the centre of the bigger sphere and the centre of that part of the smaller sphere which is still in the exterior of the other sphere.



Collective potential energy of the fusing heavy ion system $^{257}_{103}\text{No} - ^{215}_{98}\text{Am}$ as a function of the centre-of-masses distance, R . The curves (a) show V_{coll} for various eccentricities $\epsilon = 0.0, 0.2, 0.4, 0.5, 0.6$ and 0.8 with no charge polarisation, $P=0$. The change of the eccentricity has as a consequence a tremendous change in the depth of the nuclear attractive potential from about -1100 MeV to 0 MeV (a). This change is not very simple in structure. As it is seen in the detail (b) there appears a weak structure of a double humped potential in the neighbourhood of $\epsilon = 0.600$.

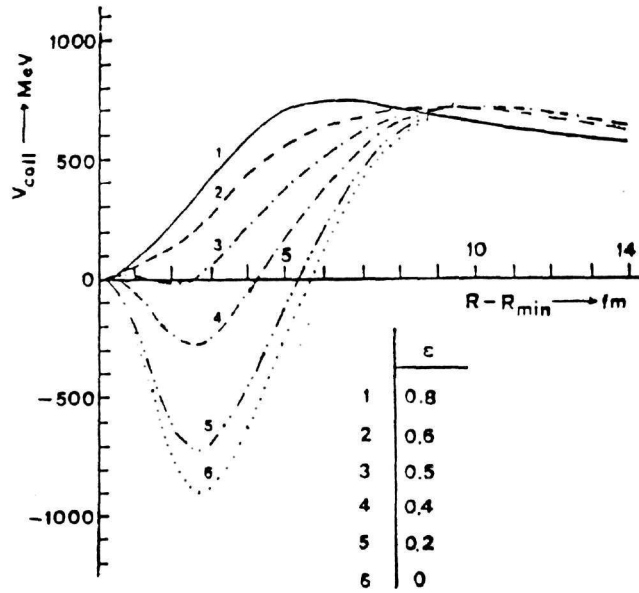


Fig. 7c.

The secondary maximum which appears at $R = R_{\min} + 6$ to 8 fm is of about 10 MeV, when the secondary minimum is (c) also situated at about $+10$ MeV. If $P \neq 0$ and $\epsilon = 0$, then the minimum of V_{coll} is of about -900 MeV. The structure of the collective potential in the upper neighbourhood of $\epsilon = 0.5$ is also shown (d). Comparing the curves in the parts (b) and (d) of the above figures it is seen that the charge polarisation strongly enhances the appearance of the secondary minimum in the collective potential energy surfaces. Since the polarisation shifts the Coulomb maximum towards smaller values \rightarrow

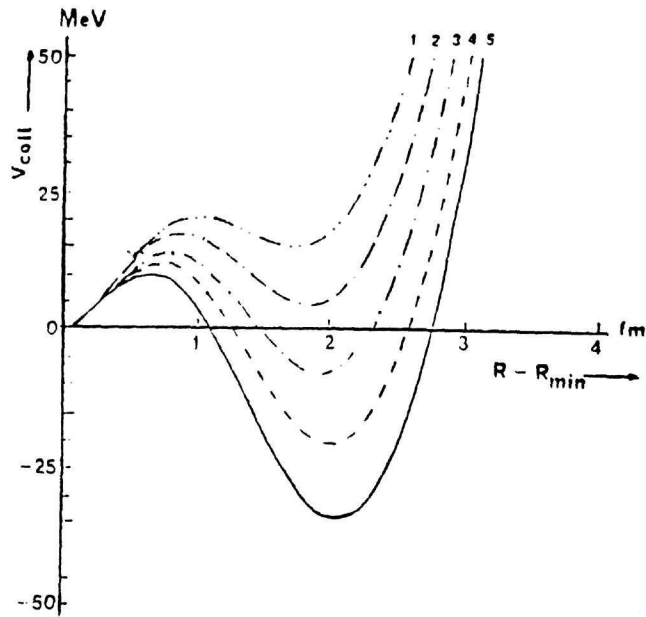


Fig. 7d.

→ of R the consequence is that the depth of the minimum is diminished as compared to the corresponding minimum without polarisation. For spherical ions and $P \neq 0$ the minima differ due just to the mentioned effect (see Fig. 6). The small energy barrier is of the order of about 10 (b) resp. 20 MeV (d), while the big one is of 650 MeV. The virtual equilibrium deformation corresponds to $R = a - \alpha + 2 \text{ fm}$, where a and α are the two large semi-axes. This equilibrium could only be realised in the process of fusion if the nucleon kinetic energies were removed by γ -emission.

$$\begin{aligned}
\text{(iii) and (iv): } V_{\text{coll}} = & (-3g^2 \cdot (\Lambda_2 - \Lambda_1'))/r_0 \cdot ((\Lambda_1 + \Lambda_2')^{1/2} c^{(\Lambda_1 + \Lambda_2')^{1/2}} \\
& - (1 + (\Lambda_1 + \Lambda_2')^{1/2} \sinh(\Lambda_1 + \Lambda_2')^{1/2}) \cdot e^{-(R+d_2(R))/r_0} / ((R+d_2(R))/r_0) \\
& + ((Z_1 + Z_2') \cdot (Z_2 - Z_1') \cdot e^2)/(R + R_c). \quad (4.26)
\end{aligned}$$

Again, the charge transfer from Λ_2 to Λ_1 is given by

$$\begin{aligned}
Z_1' = & -Z_2 + (3 \cdot Z_2 \cdot (1 - \epsilon^2)/(r_0^3 \cdot \Lambda_2)) \cdot (2(\alpha_1^2(R) + \alpha^2)/3 + (2\alpha^2 \cdot \alpha_1^2(R) \\
& - \alpha^4 - 2 \cdot \alpha_1^2(R) \cdot R^2 - 2\alpha^2 \cdot R^2 - \alpha_1^4(R))/4R + R^3/12). \quad (4.27)
\end{aligned}$$

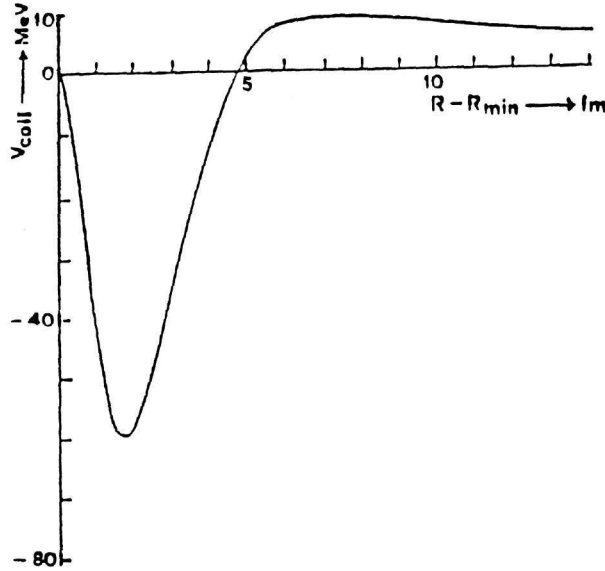
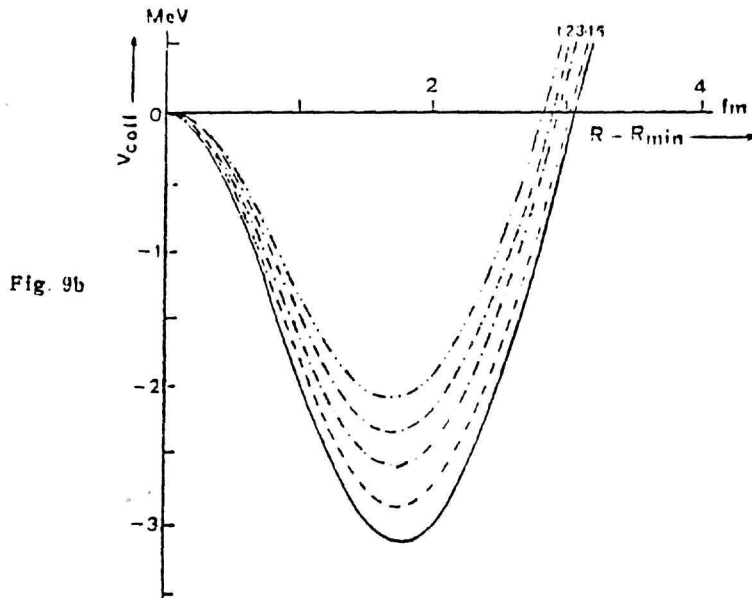
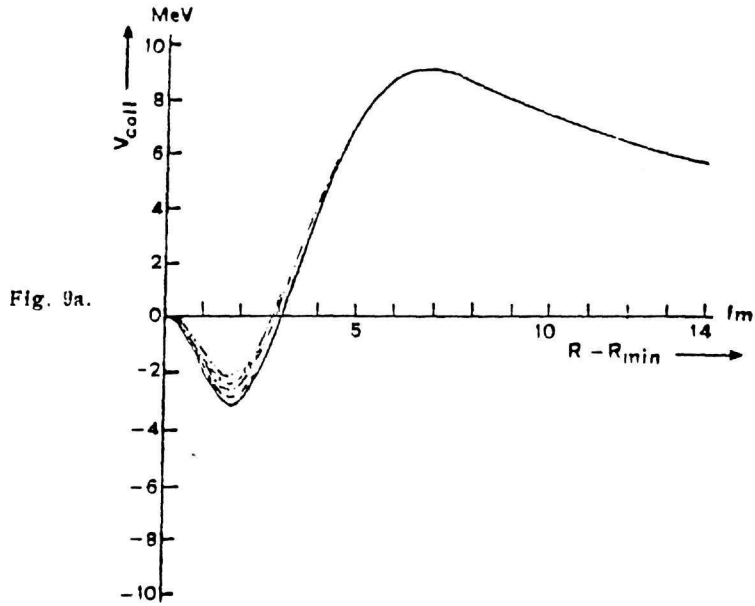


Fig. 8. Potential energy curve for the ion pair $^{20}_{10}\text{Ne} - ^{12}_6\text{C}$ with excentricity $\epsilon = 0$ and polarisation $P = 0$. In this case no secondary minimum appears.

It follows from the above expressions that the nuclear charge polarisation enhances the secondary minimum in the collective energy surface. Also the charge polarisation together with the neutron attraction may be considered as responsible for the ellipsoidal form of the colliding nuclei. Charge polarisation alone does not produce any secondary minimum in spherical nuclei. The results of the above equations are



The same as in Fig. 8 with $P=0$ and $\epsilon=0.841, 0.838, 0.834, 0.831, 0.827$ corresponding to the curves 1-5. Again in these cases no secondary minimum appears due to absence of polarisation.

shown in the Figs. 6 - 14b, where no relativity effects are considered. If the relative velocities of the two approaching ions are high, then the relativistic contraction results in a reduction of the large semi-axes of the two prolate ellipsoids. If the initial form of the nuclei is spherical, then, of course, the relativity effect consists in giving them the

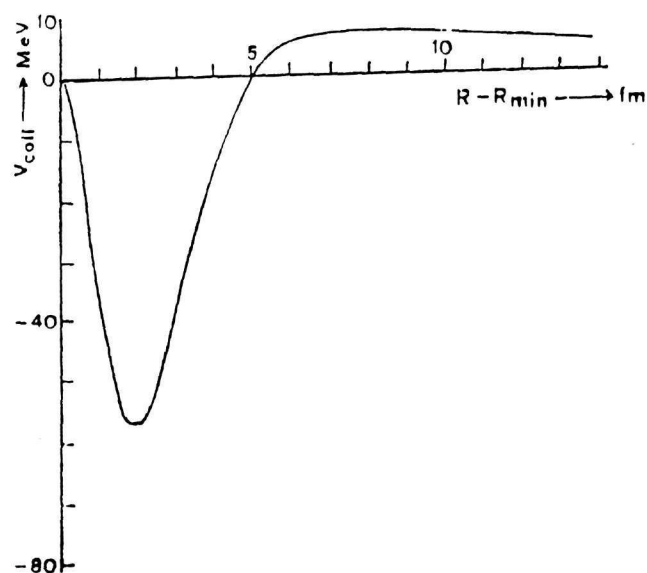


Fig. 10. The same as in Fig. 6 for the ion pair $^{20}_{10}\text{Ne} \cdot ^{12}_6\text{C}$. No secondary minimum appears due to the conditions $\epsilon=0$ despite the non-vanishing charge polarisation ($P \neq 0$).

form of the oblate ellipsoids. For prolate ellipsoids the excentricity has the expression

$$\epsilon = \sqrt{1 - (b/a)^2 (1 - \beta^2)^{-1}}, \quad (4.28)$$

where as usual (*)

$$\beta = (1 - (E_k / M \cdot c^2 + 1)^{-2})^{1/2}. \quad (4.29)$$

c is the speed of light in vacuum, E_k is the kinetic energy and M is the mass of the ion. Secondary minimum in the collective interaction appears only for particular values of the excentricity, $\epsilon(\beta)$, and it disappears completely for oblate ellipsoids as illustrated in Figs. 15a - 16b.

(*) This β should not be confused with the minor semi-axis of the ellipsoids.

Potential energy (a) as function of the centres distance of the fusing ion system $^{20}_{10}\text{Ne} - ^{12}_6\text{C}$. In contrast to the case of Fig. 7 now the ions are both deformed ($\epsilon \neq 0$) and have non-uniform charge density distributions ($P \neq 0$). The effect of this combination of parameters ($\epsilon \neq 0$, $P \neq 0$) is that the potential surface exhibits now two maxima (Coulomb) and two minima (nuclear). Due to the low numbers (A_1, Z_1) and (A_2, Z_2) the barrier heights are very small ($\sim \text{keV}$). This appears clearly in the detailed (b) curves.

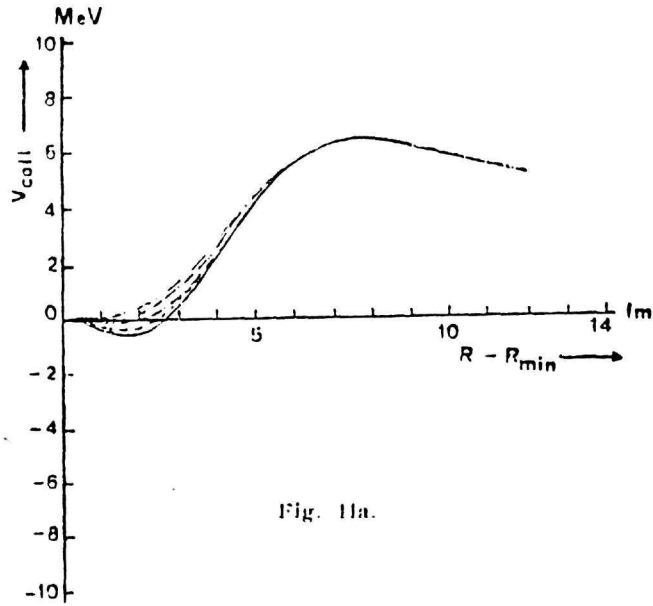


Fig. 11a.

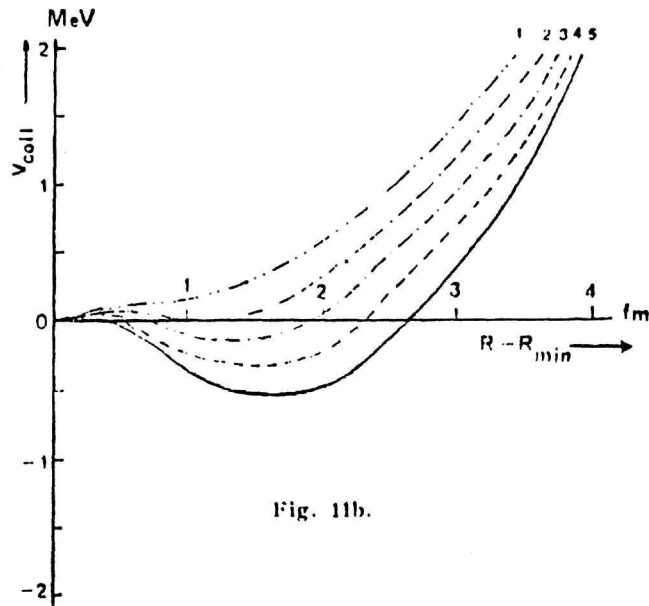
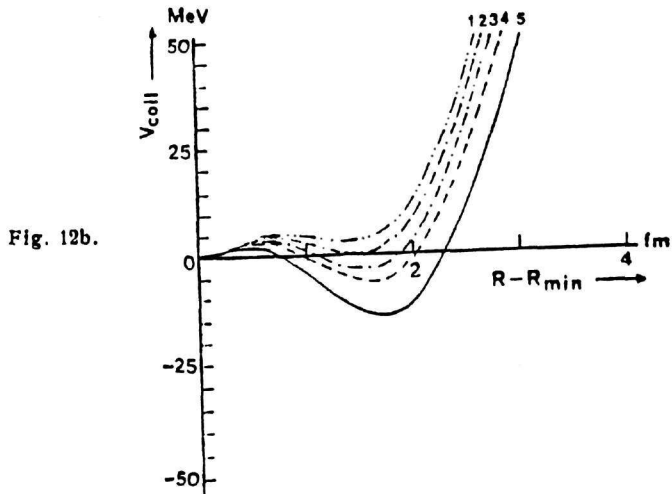
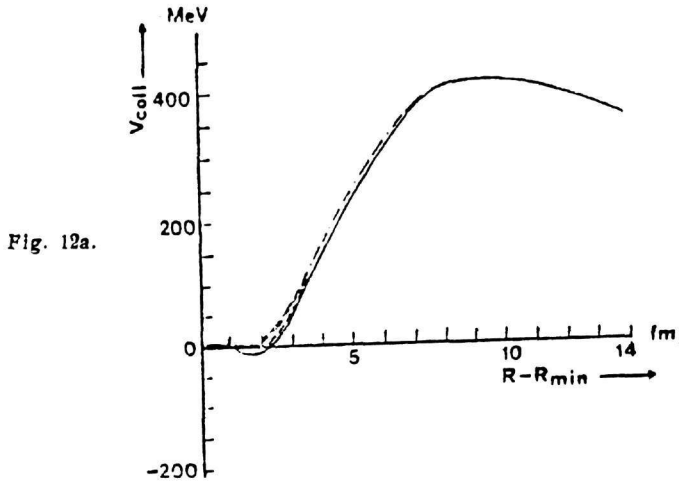
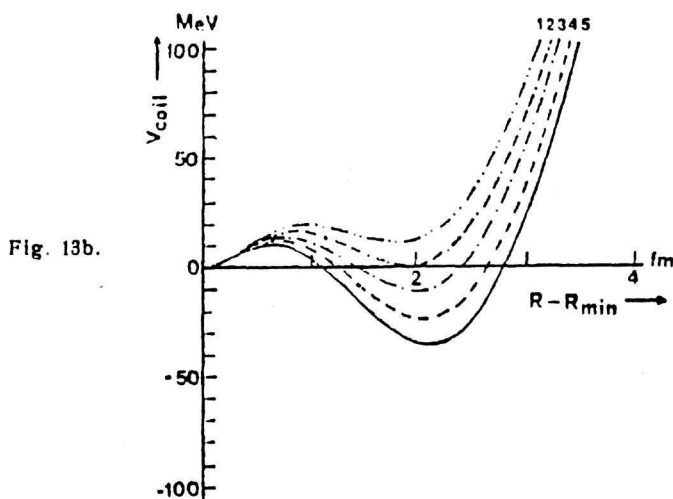
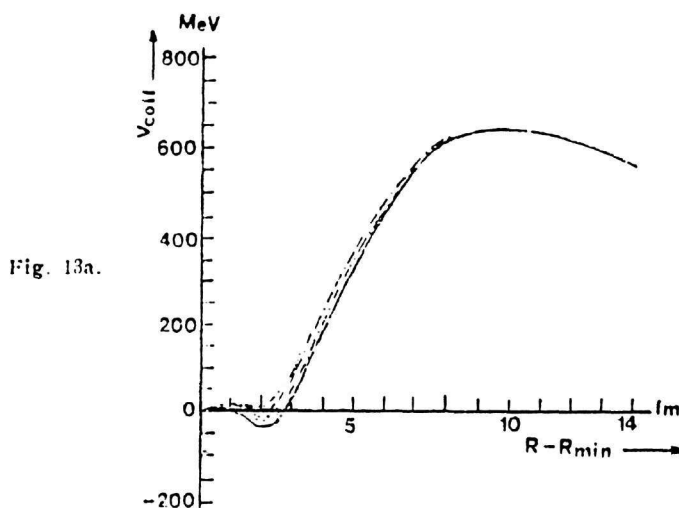


Fig. 11b.



The curves show the potential energy of the fusing system $^{235}_{92}\text{U} - ^{161}_{60}\text{Nd}$ for the excentricities (from bottom to top) $\epsilon = 0.475, 0.485, 0.490, 0.495, 0.5$ and for charge polarisation ($P \neq 0$). The doubly humped structure of the energy surface is now clear. The barrier heights now are of the order of magnitude of a few MeV as it can be seen from the detailed (b) curves.



The doubly humped character of the energy surface becomes accentuated with increasing mass and atomic numbers, A , Z . In the case of the ion system $^{243}_{94}\text{Am} - ^{241}_{95}\text{Np}$ the barrier heights are approx. 20 MeV (b) and 650 MeV (a). This behaviour of the energy surface is a consequence of the combination of the parameters $\varepsilon \neq 0$ and $P \neq 0$. The values of the excentricity are $\varepsilon = 0.517, 0.523, 0.530, 0.536, 0.593$. There is no difficulty in taking different excentricities for the two ions.

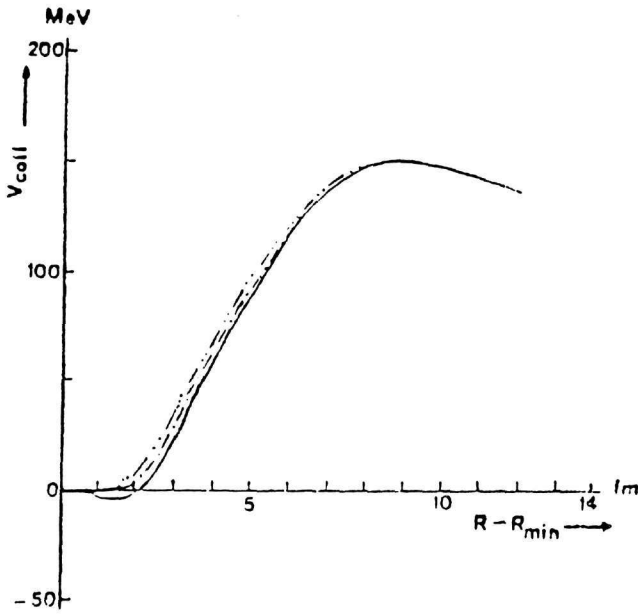


Fig. 14a.

The same (a) as in Fig. 12 for the ion system $^{166}_{62}\text{Sm} - ^{70}_{30}\text{Zn}$ for $P \neq 0$ and $\epsilon = 0.513, 0.520, 0.527, 0.534, 0.541$. It is seen from the detailed curves (b) that there is an eccentricity for which the nucleus $^{238}_{92}\text{U}$ can undergo a transition from the spherical (b) state with $R \approx 1.5 \text{ fm}$ almost without any energy consumption and indeed with the emission of about 5 MeV.

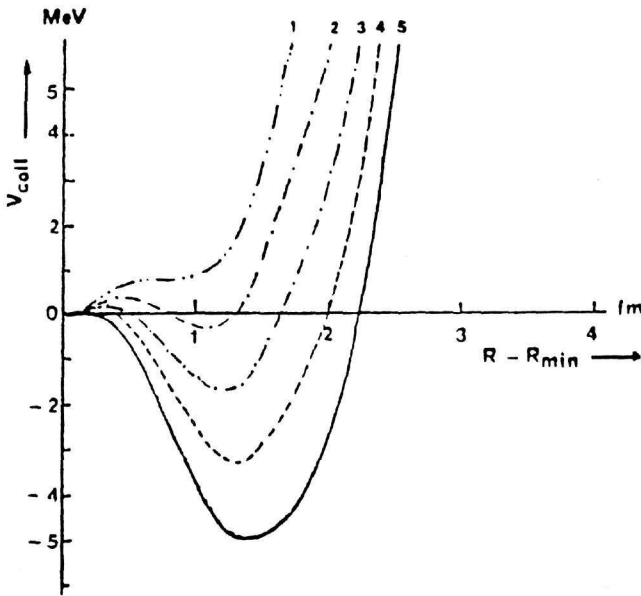


Fig. 14b.

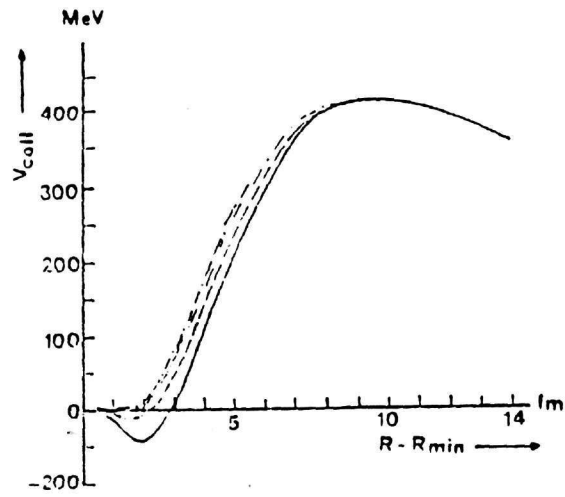


Fig. 15a.

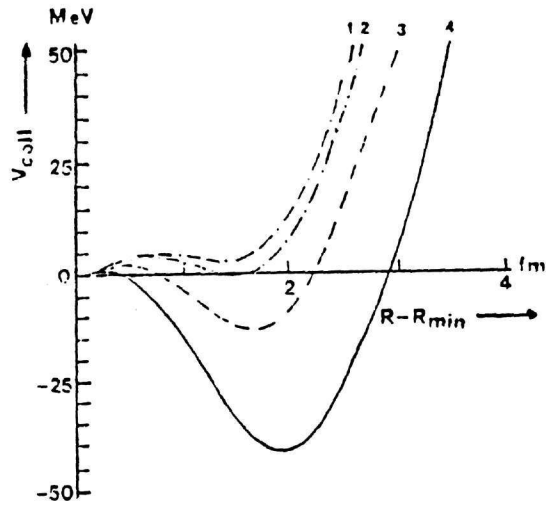


Fig. 15b.

The effect of the relativity factor $\beta = v/c$ on the potential energy curves (a) appearing during the fusion process of the heavy ions $^{235}_{92}\text{U} - ^{151}_{60}\text{Nd}$. The different curves correspond (from top to bottom) to the values $\beta = 0, 0.07, 0.14, 0.21$. It is seen in the detail that the potential energy curve is strongly suppressed towards more negative values (b). This becomes clear by comparing the curves 13b with 12b, where $\beta = 0$.

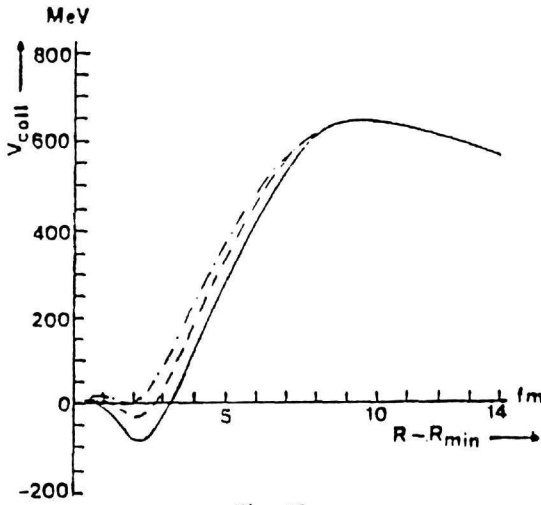


Fig. 16a.

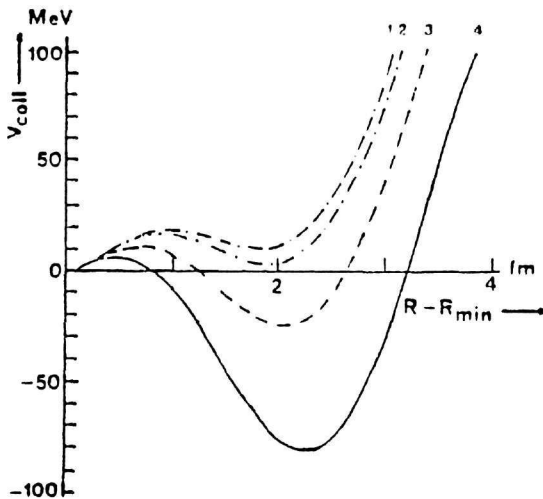


Fig. 16b.

Potential energy for the ion pair $^{215}_{95}\text{Am} - ^{241}_{95}\text{Np}$ as function of the distance with parameter the relativity factor β . The curves (from top to bottom) correspond to the values $\beta=0, 0.07, 0.14, 0.21$. The curves for the first two β -values coincide due to scale (a), whilst they are distinct in the detailed curves (b). The role of β is to deepen the potential curve for prolate ellipsoids of very high rest excentricity ($\epsilon(0) = 0.543$). On the contrary, if the rest excentricity is less than a certain value, then the effect of β is to flatten the potential curve. This demonstrates that the role of the relativity factor β is not unique but it depends on the rest excentricity of the colliding nuclei.

5. THE INFLUENCE OF THE IMPACT PARAMETER

The results described in Section 4 are valid for centric collisions, i.e., vanishing impact parameter. Since this case is not the most general one we derive here the formulas pertaining to non-zero impact parameter. For the sake of generality we consider from the beginning prolate ellipsoids. The reasons distinguishing the prolate from the oblate ellipsoids consist in that the latter do not lead to double humped potentials. They can be considered separately. The next step is to find the common volume of the two ellipsoids and calculate the nucleon transfer. To this end the coordinates of the points A, B are necessary. From Fig. 17 we find that the coordinates of these points, $A(x_A, y_A)$ and $B(x_B, y_B)$, are given as solutions of the nuclear volume conservation

$$\sigma^2 x^4 + 2\sigma\tau x^3 + \omega x^2 + 2\tau\varrho x - v^2 = 0. \quad (5.1)$$

The coefficients are functions of the centres' distance of the ellipsoids and the impact parameter, q , and have the expressions

$$\begin{aligned} \sigma &= b^2/\alpha^2 - \beta^2/\alpha^2 \\ \tau &= 2\beta^2\delta/\alpha^2 \\ \varrho &= \beta^2 - \beta^2\delta/\alpha^2 - b^2g^2 \\ v &= 2bg \\ \text{and } \omega &= \tau^2 + v^2/\alpha^2 + 2\sigma\varrho. \end{aligned}$$

The parameter δ is related to the distance of the centres and the impact parameter, q , through the relation

$$\delta = \sqrt{R^2 - q^2}. \quad (5.2)$$

The common volume $\tilde{O}(R, q)$ of the ions 1 and 2 is the sum of $\tilde{O}_1(R, q)$ and $\tilde{O}_2(R, q)$ and they can be obtained from the integral

$$\tilde{O}_1(R, q) = b^2 \int_{x_A}^{x_B} (1 - x^2/\alpha^2) [\varphi(x) - 1/2 \cdot \sin 2\varphi(x)] dx, \quad (5.3)$$

where the angle $\varphi(x)$ is given by

$$\varphi(x) = \arccos \left\{ [y_A + (y_A - y_B)(x - x_A)/(x_B - x_A)] / b \cdot \sqrt{1 - x^2/a^2} \right\} \quad (5.4)$$

and $y_B > 0$.

If $y_B < 0$, then the volume $\tilde{O}_1(R, q)$ increases by the volume $\tilde{O}_1'(R, q)$ which is calculated from the expression

$$\tilde{O}_1'(R, q) = \pi b^2 [2/3a - x_B + x_B^3/(3a^2)]. \quad (5.5)$$

More precisely we have

$$\tilde{O}_1(R, q) = \begin{cases} \tilde{\tilde{O}}_1(R, q) & ; \quad y_B > 0 \\ \tilde{\tilde{O}}_1(R, q) + \tilde{O}_1'(R, q) & ; \quad y_B < 0. \end{cases} \quad (5.6)$$

The volume \tilde{O}_1' is included inside the surface of which a plane cut is denoted in Fig. 17 by CDBC.

Similarly we find \tilde{O}_2 from (5.3) and (5.5) in the form

$$\tilde{O}_2(R, q) = \begin{cases} \tilde{\tilde{O}}_2(R, q) & ; \quad y_A < q \\ \tilde{\tilde{O}}_2(R, q) + \tilde{O}_2'(R, q) & ; \quad y_A > q. \end{cases} \quad (5.7)$$

In (5.7) the following definitions hold:

$$\tilde{\tilde{O}}_2(R, q) = \beta^2 \int_{x_A}^{x_B} [\varphi(x) - 1/2 \cdot \sin(2\varphi(x))] \cdot [1 - (x - \delta)^2/\alpha^2] dx \quad (5.8)$$

with

$$\varphi(x) = \arccos \left\{ [y_A - q - (x - x_A)(y_A - y_B)/(x_B - x_A)] / \beta \sqrt{1 - (x - \delta)^2/\alpha^2} \right\}$$

and

$$\tilde{O}_2'(R, q) = \pi \beta^2 [x_A - \delta + \alpha - x_A^3/(3\alpha^2) + (\delta - \alpha)^3/(3\alpha^2)].$$

The volume \tilde{O}'_2 is that contained inside the surface of which a plane cut is AFEA in Fig. 17.

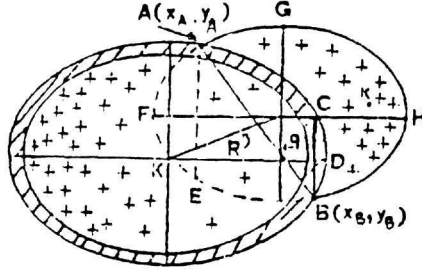


Fig. 17. Collision of two deformed nuclei with semi-axes (a, b) and (α, β) ($a > \alpha$ and $b > \beta$) and with non-vanishing impact parameter, q . The points $A(x_A, y_A)$ and $B(x_B, y_B)$ are the top and the bottom, respectively, of a plane cut of the two ellipsoids. The distance of the two centres $R = \sqrt{\delta^2 + q^2}$. The point K is the centre of mass of the part of the small ellipsoids remaining still outside the big ellipsoid. The illustrated situation of the colliding heavy ions corresponds to the case $q < \beta$. The neck is an ellipse containing the points A and B . According to our model the volume delimited by $ADBEFA$ has contributed to the increase of the big ellipsoid indicated by the shaded area. The charge polarisation is indicated qualitatively. Before complete fusion the proton charge density in the central volume of the system is considerably diminished due to the polarisation phenomenon.

Using the above results one finds for the distance K_x , where x is the centre of the volume $AGHBA$, the expression

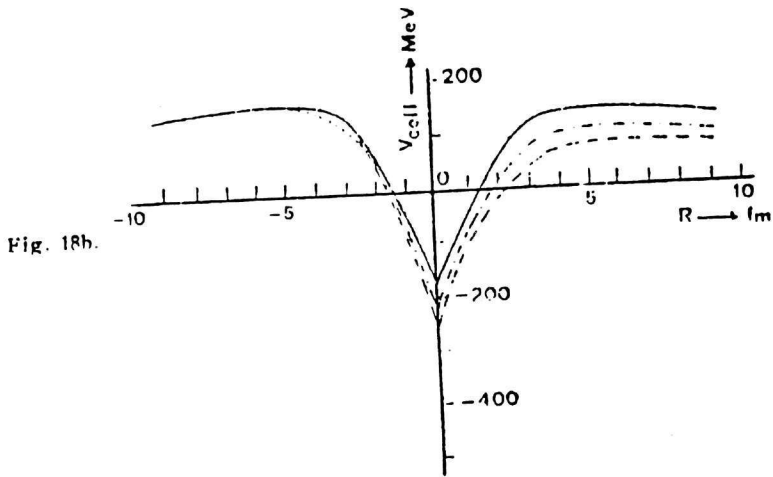
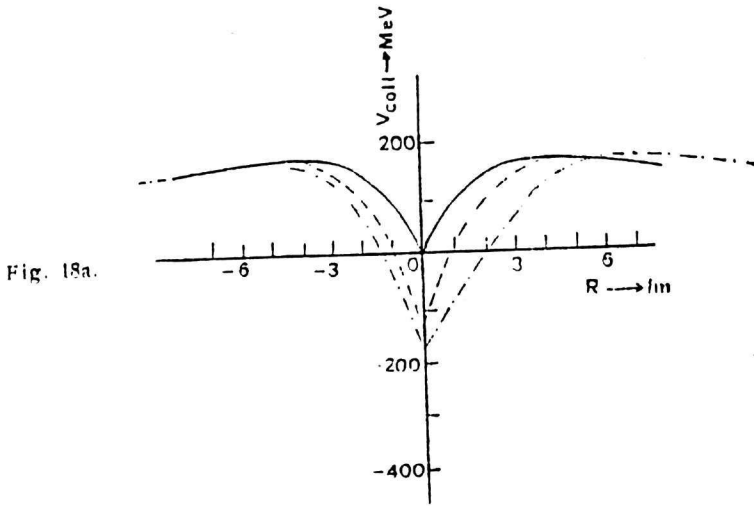
$$K_x(R, q) = [x_M^2 + y_M^2]^{1/2} \quad (5.9)$$

with

$$x_M = (I_x^a + I_x^{\alpha} + I_x^{a'} + I_x^{\alpha'}) / (V_2 - \tilde{O}_1 - \tilde{O}_2 - \tilde{O}_1' - \tilde{O}_2') + \delta \quad (5.10)$$

and

$$y_M = (I_y^a + I_y^{\alpha}) / (V_2 - \tilde{O}_1 - \tilde{O}_2 - \tilde{O}_1' - \tilde{O}_2') + q. \quad (5.11)$$



Potential energy curves for interacting heavy ions with various impact parameters during fusion or fission processes. In part (a) of the figure the potential energy curves correspond to the case in which only neutrons are transferred from the smaller to the bigger ion. It is seen that the main change in the curves appears in the region of nuclear attraction dominance, while in the Coulomb dominance region the potential energy is almost unchanged. If protons are also transferred from the smaller to the bigger ion then the change is extended to a greater region of distances as is seen in part (b) of the figure. In this particular case the two ions are mutually exchanging equal numbers of neutrons and protons, while due to the partial fusion a number of neutrons corresponding to the value of the impact parameter, q , is transferred from the smaller to the bigger nucleus. The depth of the potential curves decreases for increasing impact parameter.

The symbols in (5.10) and (5.11) are defined by

$$I_x^a = \tilde{O}_1^{-1} b^2 \int_{x_A}^{x_n} x (1 - x^2/a^2) [\varphi(x) - 1/2 \sin 2\varphi(x)] dx, \quad (5.12)$$

$$I_y^a = \tilde{O}_1^{-1} b^2 \int_{x_A}^{x_n} [y_A - (x - x_A)(y_A - y_B)/(x_B - x_A)] [\varphi(x) - 1/2 \sin(2\varphi(x))] dx, \quad (5.13)$$

$$I_x^a = \tilde{O}_2^{-1} \beta^2 \int_{x_A}^{x_n} [\varphi(x) - 1/2 \sin(2\varphi(x))] [1 - (x - \delta)^2/\alpha^2] (x - \delta) dx, \quad (5.14)$$

$$I_y^a = \tilde{O}_2^{-1} \beta^2 \int_{x_A}^{x_n} [\varphi(x) - 1/2 \sin(2\varphi(x))] [1 - (x - \delta)^2/\alpha^2] \cdot [y_A - q - (x - x_A)(y_A - y_B)/(x_B - x_A)] dx. \quad (5.15)$$

With the data obtained in the present section the collective potential according to (4.23), (4.24) and (4.26) has the form given in Fig. 18 for spherical nuclei.

6. ENTRANCE AND EXIT CHANNEL ENERGIES

In the case of elastic scattering the collective potential energy in the entry as well as in the exit channels is the same. If the scattering is inelastic the collective potential energy of the two colliding ions is, in general, different in the two channels due to the change of the nucleon states. Despite this change the error resulting from neglecting it in the collective potential energy is of minor significance.

However, when both matter and energy are transferred from the one to the other heavy ion, the difference of the collective potential energies in the entry and exit channels is so large that it cannot be ignored. In order to take it into account properly one has to make separate calculations of the collective potential energy for each channel.

This has been done in the present section. The method used consists in the following :

- (i) The impact parameter, q , and the distance of closest approach, \bar{R} , are fixed in advance. We select two ions identified by (A_1, Z_1) and (A_2, Z_2) as well as by the excentricities $\varepsilon_1, \varepsilon_2$, which for simplicity we assume to be equal, $\varepsilon_1 = \varepsilon_2$. We let these ions collide with given relative energy E_{rel} . By the procedure described in the previous sections the collective potential energy is calculated as a function of the distance, R , until this intercentre distance becomes equal to \bar{R} (Fig. 17). While $R > \bar{R}$ the collective potential is a sum of the nuclear and the Coulomb parts of the energy. The distance $R = \bar{R}$ defines the last point of the entry channel collective potential which is represented by the curve on the left of the axis of the ordinates in Fig. 18a, b.
- (ii) In the exit channel the ions do not approach each other any more but instead they recede. In the exit channel again the collective potential is the sum of the two terms as in the entry channel. However, an important difference exists now in the process of calculating it. While nucleon transfer takes place in the entry channel due to the gradually proceeding partial fusion, there is no nucleon transfer in the exit channel. Consequently, the neutron and proton numbers of the two ions are equal to those at the last stage of the fusing system in the entry channel. The numerical calculations showed that the depth and the width of the curves depend for constant A_1, A_2, Z_1, Z_2 on R, P, ε and on the impact parameter, q , of the colliding system. According to the usual convention the distance of the two centres has been given negative values.

After the above preliminary explications we proceed to a formal definition of the entrance and exit channel of the collective potentials. We consider the two interacting ions $((A_\sigma, Z_\sigma); \sigma = 1, 2)$. Let the wave function of the i -th ion be approximately given by a Slater determinant, $S^{(\alpha_\sigma)}$ as defined in Section 2. Let $\{\vec{r}_{j_\sigma}^\alpha | j_\sigma = 1, \dots, A_\sigma\}$ be the

coordinates of the nucleons. α_σ is a set of quantum numbers including A_σ , Z_σ . We write for the coordinates of the second ion nucleons

$$\vec{r}_{j_2}' = \vec{R} + \vec{r}_{j_2}^2 \text{ where } \vec{R} = \sum m_{j_2} \cdot \vec{r}_{j_2}^2 / \sum m_{j_2}$$

the CM coordinate of the second ion with respect to the CM of the first one. The expectation value $\langle \vec{R} \rangle$ is obtained from the expression

$$\langle \vec{R} (J, M, a_1, a_2, E_1, E_2) \rangle = \langle \Psi_{JM}^{(a)} | \vec{R} | \Psi_{JM}^{(a)} \rangle. \quad (6.1)$$

The wave functions $|\Psi_{JM}^{(a)}\rangle$ are defined as follows [21]:

Let I_σ, i_σ ; ($\sigma = 1, 2$) be the spin and its projection of the ions. The total spin and its projection of the ion pair are $\vec{s} = \vec{I}_1 + \vec{I}_2$ and $i_1 + i_2 = v$, where $|I_1 - I_2| \leq s \leq I_1 + I_2$. If $|S_{I_\sigma i_\sigma}^{(\alpha_\sigma)}\rangle$; $\sigma = 1, 2$ are the internal wave functions of the ions, then the total internal wave function is given by

$$\begin{aligned} \Psi_{sv}^{(a)}(\vec{r}_{11}, \dots, \vec{r}_{1A_1}, \vec{r}_{21}, \dots, \vec{r}_{2A_2}; \vec{R}) = \\ = \sum_{i_1+i_2=v} (I_1, i_1; I_2, i_2 | sv) S_{I_1 i_1}^{(\alpha_1)} S_{I_2 i_2}^{(\alpha_2)}, \end{aligned} \quad (6.2)$$

where $\{(I_1, i_1; I_2, i_2 | sv)\}$ are the Clebsch - Gordan coefficients and α_σ determines A_σ , Z_σ and all other quantum numbers of the σ -th ion.

The complete wave function is obtained by taking into account the relative motion of the ions by means of the corresponding set of relative wave functions $\{\varphi_{lm}(\vec{R}, \vec{\Omega})\}$.

The total wave function of the two ions is

$$\Psi_{JM}^{(a)} = \sum_{v+m=M} (sv; lm | JM) \varphi_{lm} \psi_{s,v}^{(a)}. \quad (6.3)$$

Since according to eq. (2.5) the matter density distribution is determined by $S_{I_\sigma i_\sigma}^{(\alpha_\sigma)}$ in each ion and consequently its shape (ε) is also determined, $\langle \vec{R} \rangle$ fixes already whether or not the two interacting ions overlap and, given their shapes, which is the volume of the overlap. If

it is assumed that the density relaxation time practically vanishes, then $\langle \vec{R} \rangle$ determines for increasing volume but constant shape ($\epsilon = \text{constant}$) of the first ion the number of nucleons already transferred to it from the second ion.

In practice, of course, the opposite way is used: For each given pair of overlapping ions with known internal wave functions, $\langle \vec{R} \rangle$ can be calculated.

The matter density can be written with the help of eqs. (2.5) and the wave function $S_{I_2 i_2}^{(a_2)}$

$$\varrho_2(\vec{r}; I_2, i_2, a_2, E_2) = \langle S_{I_2 i_2}^{(a_2)} | S_{I_2 i_2}^{(a_2)} \rangle_r, \quad (6.4)$$

where the subscript r in $\langle | \rangle_r$ means omission of integration with respect to r .

Next, suppose that there takes place continuous nucleons transfer from the ion «2» to the ion «1» with diminishing $\langle \vec{R} \rangle$. It is obvious that in this case, A_2 and Z_2 become functions of $\langle \vec{R} \rangle$. Consequently we shall write for $a_\sigma = a_\sigma(\langle \vec{R} \rangle)$. With these preliminaries we define the channel collective potential energy by the following expression:

$$V_{\text{coll}}(\langle \vec{R} \rangle; J, M, a_1(\langle \vec{R} \rangle), a_2(\langle \vec{R} \rangle); E_1, E_2) = \\ = \int_{v_2 \rightarrow 0} V_{\text{el}}(\langle \vec{R} \rangle + \vec{r}; I_1, i_1, a_1(\langle \vec{R} \rangle), E_1) \cdot \varrho_2(\vec{r}; I_2, i_2, a_2(\langle \vec{R} \rangle), E_2) \cdot d\vec{r}. \quad (6.5)$$

In eq. (6.5) the spins I_σ ; $\sigma = 1, 2$ are so added that the total spin J and projection M are as required by the expression for $\langle \vec{R} \rangle$ in eq. (6.1).

From eq. (6.5) one can obtain both the entrance or the exit channel collective potential provided one uses the entrance resp. the exit channel wave function for the relative motion of the ions in eq. (6.3).

The actual calculations in the present work have been obtained with a number of approximations to the above eq. (6.5). They are:

1) Neglect of the spins I_σ ; $\sigma = 1, 2$ in eq. (6.1) and (6.2). 2) The internal ion wave functions have been approximated by unit step functions. In this way $\langle \vec{R} \rangle$ reduces to the CM position vector of the second ion with respect to the CM of the first one.

7. THE MASS FORMULA

The procedure developed in the previous sections allows us to determine the mass of each ion in the process of fusion. In what follows we give an explicit formula for the mass which can be used in solving the equations of motion for two interacting heavy ions.

For nuclear forces of the type considered here this mass is given in proton mass units ($\lambda = m_n/m_p$) by the expression

$$\mu(R, q) = \frac{[Z_1 + \lambda \cdot (A_1 - Z_1)] \cdot [Z_2 + \lambda \cdot (A_2 - Z_2)]}{Z_1 + Z_2 + \lambda \cdot (A_1 + A_2 - Z_1 - Z_2)} \cdot \left[1 + \frac{\bar{O}(R)}{V_1} \right] \cdot \left[1 - \frac{\bar{O}(R)}{V_2} \right] \quad (7.1)$$

V_1 and V_2 are the initial volumes of the interacting ions. $\bar{O}(R)$ is given by

$$\begin{aligned} \bar{O}(R) = \pi \cdot (1 - \epsilon^2) \cdot \left[\frac{2}{3} \cdot (\alpha_1^3(R) + \alpha^3) + \frac{1}{4} R \cdot (2\alpha^2 \cdot \alpha_1^2(R) - \right. \\ \left. - 2 \cdot \alpha_1^2(R) \cdot R^2 - 2\alpha^2 \cdot R^2 - \alpha_1^4(R) - \alpha^4) + R^3/12 \right] \end{aligned} \quad (7.2)$$

The form of $\mu(R, q)$ is given in Fig. 19.

8. CONCLUSIONS AND DISCUSSION

The results presented in the foregoing sections are based mainly on the single-particle potential derived from the scalar π -meson field theory. The most striking feature of this potential is its structure as function of A and Z . It is noted that for increasing Z there does not only decrease the depth for protons but also the slope of the curve $V(r)$ in the neighbourhood of $r=0$ changes sign for values of the proton number larger than a certain value Z_0 . The collective potential energy surface shows a behaviour which strongly depends on the shape defor-

mation of the interacting heavy ions. Also the charge polarisation plays a primordial role in the enhancement of the secondary minimum in the neighbourhood of vanishing deformation. For spherically symmetric nuclei the charge polarisation is not sufficient to produce the secondary minimum. Similarly, the shape deformation without charge polarisation does not lead to a secondary minimum in nuclei with medium mass

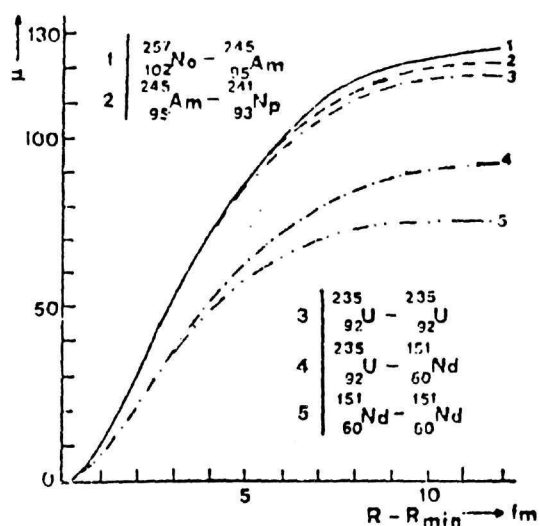


Fig. 19a.

Change of mass for the collective motion during fusion or fission processes. In the part (a) of the figure the curves show the variation of the mass with the distance of the mass centres for the case of the complete fusion or fission in a form corresponding to zero impact parameter, $q=0$, for various ion pairs.

number. The depth of the secondary minimum is a function of the excentricity the maximum being of the order of 10 MeV in heavy nuclei, a value strongly depending on the coupling constant g . One of the most important results is the prediction that certain spherical nuclei may undergo radiative transitions ($\sim 5\text{MeV}$) to shape deformed and charge polarised states. Another interesting feature of the collective potential is that for highly relativistic energies there does not show

In the second part (b) of the figure the mass is given for various values of the impact parameter in the case of the ion pair $^{138}_{56}\text{Ba} - ^{97}_{36}\text{Kr}$ for both neutron (b) and proton (c) transfer. The left-hand side of the curve gives the variation of the mass in the entrance channel while the right-hand side gives the mass in the exit channel. In the exit channel the mass is almost constant due to the detachment of the ions. The mass variation becomes stronger for decreasing impact parameter. The negative values of R correspond to the entrance channel of the reaction.

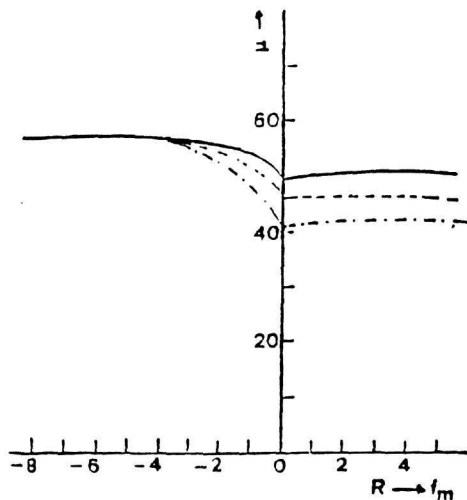


Fig. 19b.

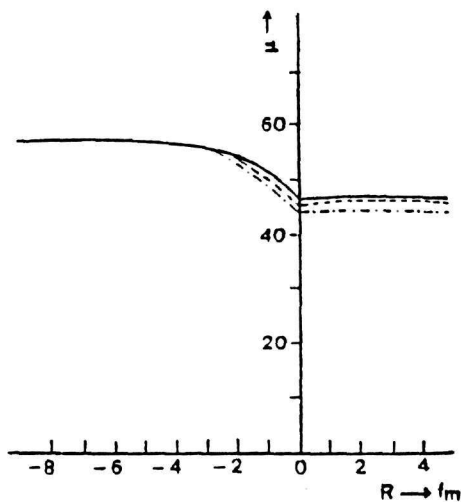


Fig. 19c.

any secondary minimum. The reason for this fact is that the combination of excentricity and charge polarisation which seem to be physically mutually inclusive, is spoiled. It is also noted that the mass of the interacting heavy ion system shows the expected behaviour. At very large distances it takes the value of the reduced mass of a two particle system whilst at very small distances it vanishes completely. Concerning the accuracy of the theory we point out that two kinds of approximations have been adopted: In the place of the nuclear radius we have used the approximate expression $a = r_0 A^{1/3}$, where for r_0 the value $r_0 = 1.2$ fm has been used. We have done no attempt to optimise the value of r_0 . However, there are indications that the dependence on r_0 may become crucial in some cases concerning the nucleon transfer criterion. The evaluation of this criterion shows that nucleon transfer proceeds from lighter to heavier nuclei, if the mass number is bigger than a critical value. We took the point of view that the nucleons outside the bigger ion interact collectively with the nucleons inside of it from the effective distance of their centre of mass. A similar point of view has been taken also in the calculation of the nuclear charge polarisation.

We have tried to keep the calculations analytical as far as possible. If use of the computer is made for the calculation of certain multiple integrals, an increase of the accuracy may appear but as we believe it will not change substantially the shape of the obtained curves.

References

- [1] J. Maruhn and W. Greiner, Phys. Rev. Lett. **32** (1978) 548
- [2] M. Bolsterli, E. O. Fiset, J. R. Nix and J. L. Norton, Phys. Rev. **C5** (1972) 1058
- [3] W. Noerenberg, Phys. Rev. **C5** (1972) 2020
- [4] M. Lefort, Phys. Rev. **C12** (1975) 686
- [5] M. G. Mustafa and H. W. Schmitt, Phys. Rev. **C8** (1973) 1924
- [6] K. T. R. Davies, A. J. Sierk and J. R. Nix, Phys. Rev. **C13** (1976) 12
- [7] L. G. Moretto, Phys. Lett. **38B** (1972) 393
- [8] M. T. Magda, A. Sandulescu, D. G. Popescu and W. Greiner, J. Phys. G: Nucl. Phys. **6** (1980) 221
- [9] M. Wakai and A. Faessler, Nucl. Phys. **A307** (1978) 349
- [10] J. P. Blocki, J. Randrup, W. J. Swiateki and C. F. Tsang, Ann. Phys. **105** (1977) 427
- [11] J. Randrup, Nucl. Phys. **A307** (1978) 319
- [12] W. D. Myers, Nucl. Phys. **A204** (1973) 465
- [13] P. R. Christensen and A. Winter, Phys. **65B** (1976) 19
- [14] J. R. Birkelung and J. R. Huizenga, Symposium on Heavy-Ion Elastic Scattering, October 25-26, 1977, Rochester, NY
- [15] J. R. Nix, Ann. Rev. Nucl. Sci. **5** (1972) 65
- [16] H. Wojciechowski, N. B. J. Tannous, R. H. Davis, D. Stanley, M. Golin and F. Petrovich, Phys. Rev. **C17** (1978) 2126
- [17] S. L. Tabor, D. F. Geesaman, W. Hennig, D. G. Kovar, K. E. Rehm and F. M. Prosser Jr., Phys. Rev. **C17** (1978) 2136
- [18] C. Syros, a) Collective Energy for Heavy Ion Nuclear Reactions, in Proceedings of the 1981 Conference of the European Physical Society/ Nuclear Physics Division, on "Nuclear and Atomic Physics with Heavy Ions" (Bucharest, 1982),
b) Charge Polarization and Interaction Energy of Heavy Ions, Amsterdam Conference, August/September 1982
- [19] V. M. Strutinski, Nucl. Phys. **A95** (1967) 420
- [20] V. M. Strutinski, Nucl. Phys. **A122** (1968) 1
- [21] J. Humblet and L. Rosenfeld, Nucl. Phys. **26** (1961) 529